

Understanding how Differentially Private Generative Models Spend their Privacy Budget

Georgi Ganev^{1,2}, Kai Xu³, and Emiliano De Cristofaro¹

¹UCL ²Hazy ³Amazon

Abstract

Generative models trained with Differential Privacy (DP) are increasingly used to produce synthetic data while reducing privacy risks. Navigating their specific privacy-utility trade-offs makes it challenging to determine which models would work best for specific settings/tasks. In this paper, we fill this gap in the context of tabular data by analyzing how DP generative models distribute privacy budgets across rows and columns, arguably the main source of utility degradation. We examine the main factors contributing to how privacy budgets are spent, including underlying modeling techniques, DP mechanisms, and data dimensionality.

Our extensive evaluation of both graphical and deep generative models sheds light on the distinctive features that render them suitable for different settings and tasks. We show that graphical models distribute the privacy budget horizontally and thus cannot handle relatively wide datasets while the performance on the task they were optimized for monotonically increases with more data. Deep generative models spend their budget per iteration, so their behavior is less predictable with varying dataset dimensions but could perform better if trained on more features. Also, low levels of privacy ($\epsilon \geq 100$) could help some models generalize, achieving better results than without applying DP.

1 Introduction

Techniques to create synthetic data from generative models have been increasingly the focus of researchers [43], governments [14, 60, 61, 63], regulators [42], and industry alike [75]. Alas, training these models without privacy guarantees can lead to overfitting and/or memorization of individual records [17, 79], which, in turn, enables attacks like membership and attribute inference [20, 40, 41]. Therefore, models should be trained to satisfy Differential Privacy (DP) [28], using noisy/random mechanisms to provably minimize the contribution, and thus the exposure, of any single data point.

Hay et al. [38] show that the more complex DP algorithms become, the harder it is to predict their performance and grasp for which applications/settings they would work well. Alas, in the context of generative models, our understanding is limited to a few experimental analyses performed on relatively small (i.e., involving a few thousand records with a dozen features) datasets, rarely beyond a single evaluation

metric. Furthermore, it is unclear if/how the models scale to larger and more realistic datasets, even though several companies, as part of their product offerings, claim they can scale and run in minutes even for very large datasets [4, 22, 35, 71].

Overall, we often do not know what the performance of generative models on downstream tasks would be vis-à-vis wider/taller data dimensions and decreasing privacy budgets. The conventional wisdom is that computations/methods satisfying DP become more accurate with more training data and less so with stricter privacy guarantees. However, in some cases, increasing the dataset size or the number of training iterations makes deep learning classifiers worse when optimized with DP-SGD [59]. Conversely, satisfying a small degree of DP ($\epsilon \geq 100$) seems to improve the performance of CNNs on limited data [66] and GANs for imbalanced data [31], while effectively defending against reconstruction attacks [36, 39] even with strong adversaries [12].

Technical Roadmap. With this motivation in mind, in this paper, we set to study the *effects* of i) different generative models, ii) various DP mechanisms, and iii) the dimensionality of training data vis-à-vis privacy-utility tradeoffs in the context of synthetic (tabular) data. We do so by analyzing how DP generative models distribute their privacy budget across rows and columns, while varying their number, as “spending the budget” through noisy/random mechanisms is where utility degradation mainly comes from. This allows us to evaluate how the choice of model and DP mechanism ultimately affects the quality of the synthetic data for downstream tasks—e.g., capturing simple distributions, maintaining high similarity, clustering, and classification.

We study both graphical and deep generative state-of-the-art models, experimenting with PrivBayes [82] and MST [55] for the former and DP-WGAN [6] and PATE-GAN [44] for the latter. In total, we train over 19,000 models on realistic datasets with dimensionality at least 10x larger than previous studies (spanning 1,024 vs. 100 columns [56, 74]).

To understand the effects of model/DP/dataset dimensions, we first need to find out i) how *scalable* DP generative models are in terms of the dimensions of the dataset and ii) whether or not DP generative models distribute their privacy budgets in a similar way. We show that the graphical models distribute their privacy budget per column, cannot scale to many features (256 for PrivBayes and 128 for MST at most) as they suffer from the curse of dimensionality, and increasing the number of rows does not affect the training time. Deep

generative models spend their budget per training iteration and can handle much wider datasets but become slower with more data. These findings cast doubts on claims that models can be trained and data generated at scale within minutes [4, 22, 35, 71].

Main Findings. In summary, among other results, our analysis shows that:

1. Graphical and deep generative models are better suited for opposite settings – the former for data with a limited number of features and simple tasks while the latter for larger datasets and more complex problems.
2. Within the same kind of models, different algorithms behave differently. For instance, PrivBayes is the only model with fairly consistent behavior. Its performance monotonically degrades when a stricter privacy budget is imposed, or the number of columns increases, while more data counters these effects. It is more scalable than MST and can separate signal from noise in the clustering task.
3. MST performs best at capturing simple statistics and has the best privacy-utility tradeoff for this task. Also, with limited data, it benefits from a small degree of privacy ($\epsilon \geq 100$). Increasing the number of rows too much, however, can cause MST to overfit and degrade its performance on more complex tasks (e.g., classification or preserving pairwise correlations). Also, it often underperforms alternative models, in contradiction to previous research claiming MST to be the most effective, scalable, and superior model overall [53, 61, 74].
4. The GANs exhibit more variable behaviors with different dataset dimensions. While they are not as competitive on simple tasks, PATE-GAN is, in fact, better suited to more complex tasks and often outperforms both graphical models, which refutes arguments that GANs are unsuitable for tabular data [56, 74]. Also, PATE-GAN improves with more features and is consistently better than DP-WGAN.
5. Notably, and perhaps unexpectedly, for all models, we find scenarios for which adding more data or relaxing the privacy constraints (increasing ϵ) could actually hurt performance. This might appear counterintuitive but might, in fact, exemplify the difficulty of deploying stable and consistent DP synthetic data models.

Overall, we are confident that our work will assist researchers and practitioners deploying DP synthetic data techniques in understanding the tradeoffs and navigating through the best candidate models vis-à-vis the dataset features, desired privacy levels, and downstream tasks.

2 Background and Related Work

In this section, we review related work on Differential Privacy and data dimensionality for queries, classification mod-

els, and generative models. In Appendix A, we provide additional background information on DP, synthetic data generation, and DP generative models.

Notation. In the rest of the paper, we use n to denote the number of rows and d and the number of columns of the real dataset. Also, ϵ denotes the privacy budget and δ the probability of failure in a DP mechanism (see Equation 1 in Appendix A).

DP Queries and Data Dimensionality. Hay et al. [38] benchmark 15 DP algorithms for range queries over 1 and 2-dimensional datasets, showing that increasing values of n reduce error. For small n , data-dependent algorithms tend to perform better; for large n , data-independent algorithms dominate. For (more complex) predicate counting queries and higher dimensional data, McKenna et al. [54] propose a method with consistent utility improvements and show that increasing d results in more significant errors. However, they experiment with datasets with at most 15 features, and their model struggles to scale beyond 30-dimensional datasets.

DP Classifiers and Data Dimensionality. For standard predictive models, more data and longer training usually lead to better performance, i.e., lower loss/better classification on the training set. This also holds for DP logistic regression learned via empirical risk minimization and objective perturbation [19]: for large n , the cost function tends to the non-private one, and while the scale of the noise is independent of d , there is a linear shift to the objective function that does not affect the optimization if it is strongly peaked [7]. However, this does not always hold; for instance, methods based on iterative training like DP-SGD trade off training steps and noise added per iteration [59].

DP Generative Models and Data Dimensionality. Unlike query answering and classification tasks, the output of generative models lives in a high-dimensional space. Thus, it likely has much higher sensitivity, making its analysis a lot more complex. Furthermore, private synthetic data generation is computationally challenging (exponential in d in the worst-case scenario, i.e., all 2-way marginals are preserved [27, 77]). Nevertheless, worst-case complexities do not rule out practical algorithms (such as those introduced in Appendix B); indeed, if *most*, rather than all, correlations are preserved, one can build computationally efficient algorithms [15].

Since there is no “one-size-fits-all” DP synthetic data generation method, Jordon et al. [43] highlight the need to empirically assess the privacy and fidelity of the data on a *per-case* basis. While [38] provides a set of standardized evaluation principles for DP query answering algorithms, including varying domain size, scale, and shape, no similar study focuses on synthetic data generation. In fact, current frameworks for synthetic data evaluation [9] do not consider varying n and d as essential factors, and benchmark studies [74] do not consider datasets with more than 41 features.

Moreover, to our knowledge, state-of-the-art graphical models have not been evaluated on datasets with more than 100 dimensions. Takagi et al. [72] argue that PrivBayes

DP Model	Model Type	DP Mechanism	Max d
Independent	Marginal	Laplace	1,024
PrivBayes	Graphical	Exponential + Laplace	256
MST	Graphical	Exponential + Gaussian	128
DP-WGAN	Deep Learning	DP-SGD	1,024
PATE-GAN	Deep Learning	PATE	1,024

Table 1: DP Generative Models Analyzed.

only performs well for datasets with simple dependencies and a few features, while MST cannot reconstruct the essential information from limited information (i.e., 1 and 2-way marginals) required for more complex classification tasks. Finally, Li, Cao, and Yao [46] observe that the two models are usually tested on tabular datasets with dozens of dimensions and claim that they still suffer from the curse of dimensionality.

Overall, our work aims to bridge these gaps through an extensive empirical evaluation, testing both graphical models and deep generative models on diverse dataset sizes and shapes as well as a variety of downstream tasks with different complexity.

3 Preliminaries

In this section, we introduce the datasets and the DP generative models used in our evaluation and analyze the steps in which they distribute their privacy budgets.

3.1 DP Generative Models

Table 1 lists the DP generative models used in our analysis. In addition to Independent (baseline marginal model), we focus on two types of generative approaches, graphical models (PrivBayes and MST) and GANs (DP-WGAN and PATE-GAN). The former model the joint distribution by breaking it down to explicit lower-dimensional marginals. The latter approximate the distribution implicitly by iteratively optimizing two competing neural networks until reaching an equilibrium: a generator, creating synthetic data from noise, and a discriminator, separating real from synthetic points.

We select these models as they are well-studied and tested, have reliable open-source implementations, and have proven to be among the top-performing solutions in practice, winning both the DP Synthetic [61] and The Unlinkable Data Challenge [62] competitions run by NIST. Also, they rely on different modeling techniques and DP mechanisms. More details on the models are in Appendix B.

3.2 Privacy Analysis

The two types of models substantially differ from each other from a DP perspective, e.g., what DP mechanisms they use, how they distribute their budgets, what factors cause more considerable expenditures, etc. The graphical models rely on the “select-measure-generate” paradigm, i.e., the first two steps are: 1) select a collection of low-dimensional marginals, and 2) measure them with a noise addition mech-

anism. Naturally, as d increases, the privacy budget needs to be distributed among more marginals, potentially leading to more noisy measurements. By increasing n , however, we could expect to decrease the per-measurement sensitivity and thus resulting in more accurate estimations.

As for GANs, one of the most widely used approaches is to train them iteratively using mini-batches based on DP-SGD. For fixed-networks architectures, increasing d should not be a major factor as that only affects the discriminator’s input and the generator’s output layers. Analyzing the effect of increasing n is more complicated. On the one hand, more (clean and diverse) training data is better for the model as that helps it generalize; on the other hand, more iterations could make the model worse as a lower privacy budget is used per iteration, and so the scale of the noise goes up [59].

Independent. Unlike the other four models, this is the only one that distributes its DP budget *independently* of the data. It always selects the same marginals (all columns) and uses the same amount of budget to get every noisy marginal, ϵ/d .

PrivBayes and MST. In total, PrivBayes measures approx. d 4-dimensional (if the network degree is three) noisy distributions, each of which has allocated $\epsilon/2d$. The MST measurement step has a few advantages over PrivBayes: i) it devotes more budget to it (2/3 vs. 1/2); ii) it models structural zeros in the distribution (areas with negligible probability); iii) it uses the Gaussian mechanism, which has better bounds than Laplace; and iv) even though in total it measures more marginals (approx. $2d$ 1 or 2-way vs. d 4-way), their dimensionality is lower, which means that the noise could be distributed more efficiently. However, it requires more computations, potentially leading to slower run times as Private-PGM is called twice, namely, in the selection and generation steps.

DP-WGAN and PATE-GAN. In DP-WGAN, the privacy budget is not directly computed but estimated using the moments accountant method [1]. Unlike graphical models, DP-WGAN spends its privacy budget iteratively through DP-SGD. PATE-GAN also relies on the moments accountant. An advantage over DP-WGAN is that noise is not added directly to the gradients but to the vote of the teacher-discriminators. Furthermore, the accountant in PATE-GAN would attribute a lower privacy cost to accessing noisy aggregations (from the teacher-discriminators) with stronger consensus as a single teacher/data point would have a lower influence on the final vote.

3.3 Datasets

For our experiments, we create four datasets based on the normal distribution (*Eye Gauss*, *Corr Gauss*, *Mix Gauss Unsup*, *Mix Gauss Sup*), associated with progressively more difficult tasks in order to test whether generative models can capture replicate them appropriately. We also include four datasets, two high-dimensional tabular ones (*Covertime* and *Connect 4*) and two common ones (*Census* and *MNIST*) to be consistent with previous work [31, 66, 74]. A summary is in Table 2, and more details, along with the dimension ranges and associated tasks, are included in Appendix C.

Dataset	Max n	Max d	Downstream Task Evaluated
<i>Eye Gauss</i>	128k	1,024	Statistics: Mean (Fig. 5) and Correlation (Fig. 6), PCA (Fig. 14, 15)
<i>Corr Gauss</i>	128k	1,024	Statistics: Mean (Fig. 7) and Correlation (Fig. 1, 8), PCA (Fig. 16, 17)
<i>Mix Gauss Unsup.</i>	128k	1,024	PCA (Fig. 18, 19), Clustering (Fig. 13)
<i>Mix Gauss Sup.</i>	128k	1,024	PCA (Fig. 20, 21), Classification (Fig. 22)
<i>Coverttype</i>	465k	55	Similarity: Marginal and Mutual information (Fig. 9)
<i>Census</i>	199k	41	Similarity: Marginal and Mutual information (Fig. 2, 10, 12), Classification (Fig. 3a, 4, 23)
<i>Connect 4</i>	54k	43	Classification (Fig. 24)
<i>MNIST</i>	60k	784	Classification (Fig. 3b, 3c)

Table 2: Datasets and downstream tasks used in our experiments.

DP Model \downarrow $d \rightarrow$	8	16	32	64	128	256	512	1,024
Independent	0.00	0.01	0.01	0.03	0.08	0.22	0.89	3.03
PrivBayes	0.01	0.02	0.06	0.26	2.29	34.15		
MST	0.75	1.55	3.23	7.71	35.90			
DP-WGAN	0.50	0.58	0.76	1.24	3.53	6.47	12.52	23.97
PATE-GAN	0.65	0.68	0.76	0.94	1.40	2.13	4.09	10.38

Table 3: Run time (in minutes) of the model’s fitting step for DP generative models, on *Corr Gauss*, with varying d and $n = 16k$.

4 Experimental Evaluation

In this section, we present our experimental evaluation involving four DP generative models (plus a baseline model) and eight datasets over several downstream tasks – scalability, statistics, similarity, and classification (a description of all tasks could be found in Appendix D).¹

For all generative models and all privacy budgets, we train the model $m = 5$ times and generate $s = 5$ synthetic datasets, which yields 25 synthetic datasets for each reported point in the plots. Besides varying the dataset dimensions (as discussed in Appendix C), we also vary the privacy budget ϵ in the range $\{0.01, 0.1, 1, 10, 100, 1k, 10k, \infty\}$. In total, we train 19k generative models and generate 95k synthetic datasets. A summary of all our experiments is reported in Table 2.

4.1 Scalability

In Table 3, we report the runtimes of the models’ fitting step on *Corr Gauss* with varying d . In Appendix E.1, we also report the runtimes of the fitting and generation (for a fitted model) steps while varying n and d (see Tables 4–6). All experiments are run on an AWS instance (m4.4xlarge) with a 2.4GHz Intel Xeon E5-2676 v3 (Haswell) processor, 16 vCPUs, and 64GB RAM. We opt to set very practical time constraints to stress test scalability *claims* from commercial players [4, 22, 35, 71]; specifically, we discard models taking longer than 60 minutes to train. (This also allows us to maintain a reasonable amount of models to test.)

The graphical models scale polynomially with d and quickly approach the 60 minutes limit — it takes PrivBayes 35 minutes to fit on a 256-dimensional dataset and MST 36 minutes on 128 dimensions while increasing n is barely a

factor. On the other hand, increasing either d or n slows the GANs — the former due to the increase of the first and last layers of, respectively, the discriminator and generator and the latter due to the increased number of iterations (we fix the number of epochs instead). PATE-GAN is more efficient than DP-WGAN as PATE only adds noise to the teacher-discriminator votes, while DP-SGD clips the per instance gradients and adds noise to all discriminator layers. For all models apart from Independent, the generation step only takes a fraction of the training time.

4.2 Statistics

We report the off-diagonal pairwise correlation across all columns of *Corr Gauss* with varying n and d in Fig. 1. We visualize the remaining statistics for *Eye Gauss* and *Corr Gauss* in Appendix E.2 (see Fig. 5, 7 for mean and Fig. 6, 8 for other pairwise correlation).

Overall, MST captures the distributions best, especially the mean and other pairwise correlations, and it is the least sensitive to changing n and d . The off-diagonal pairwise correlation in Fig. 1 shows that, for $n \leq 4k$, the correlation score *improves* when privacy is applied and is above the “no-DP” values for $\epsilon \geq 10$. In other words, DP acts as regularization when the model has insufficient data to capture the distribution. To our knowledge, this is the first finding of this kind for non-deep learning DP model; previous studies were limited to CNNs [66] and GANs [31], which are neural networks relying on, respectively, DP-SGD and PATE. Note that MST does not scale beyond 128 features.

PrivBayes can handle wider datasets, up to 256 columns. It performs as expected, as mean and other pairwise correlations stay close to 0 for all n and d for both datasets. However, for off-diagonal pairwise correlation (see Fig. 1), there is a monotonic improvement with increasing n and deterioration with increasing d , reaching the baseline levels of Inde-

¹Due to space constraints, the PCA and clustering evaluations on all *Gauss* datasets are presented in E.4.

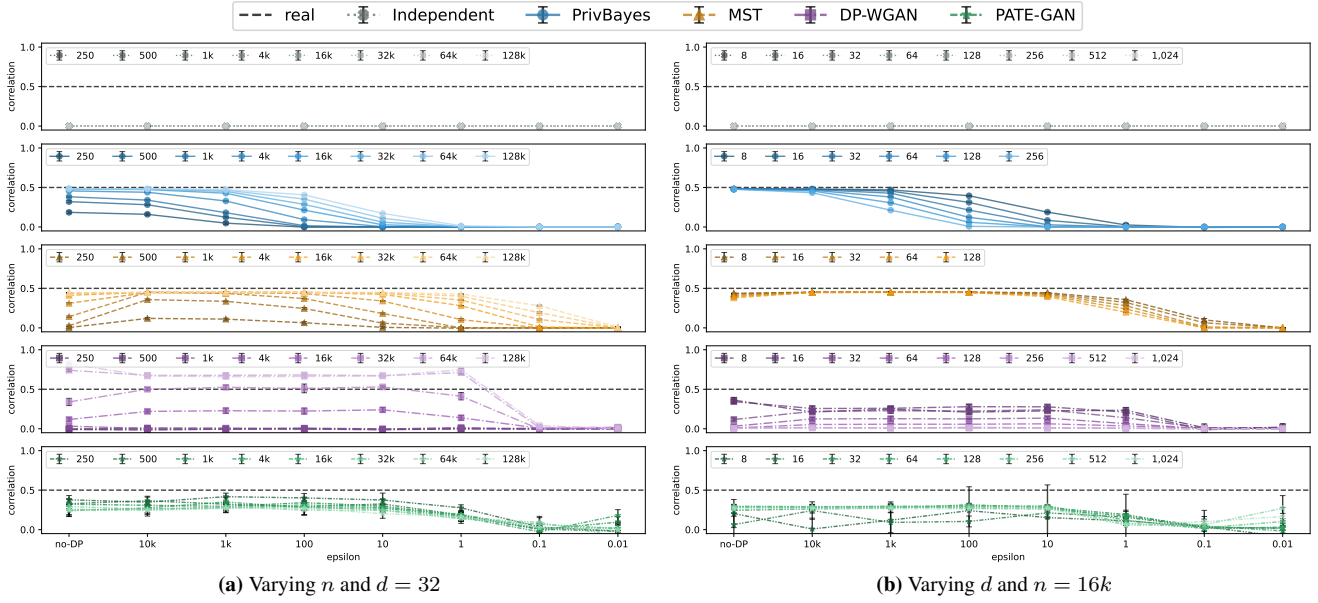


Figure 1: Off-diagonal pairwise correlation for different ϵ levels, on *Corr Gauss*, varying n and d .

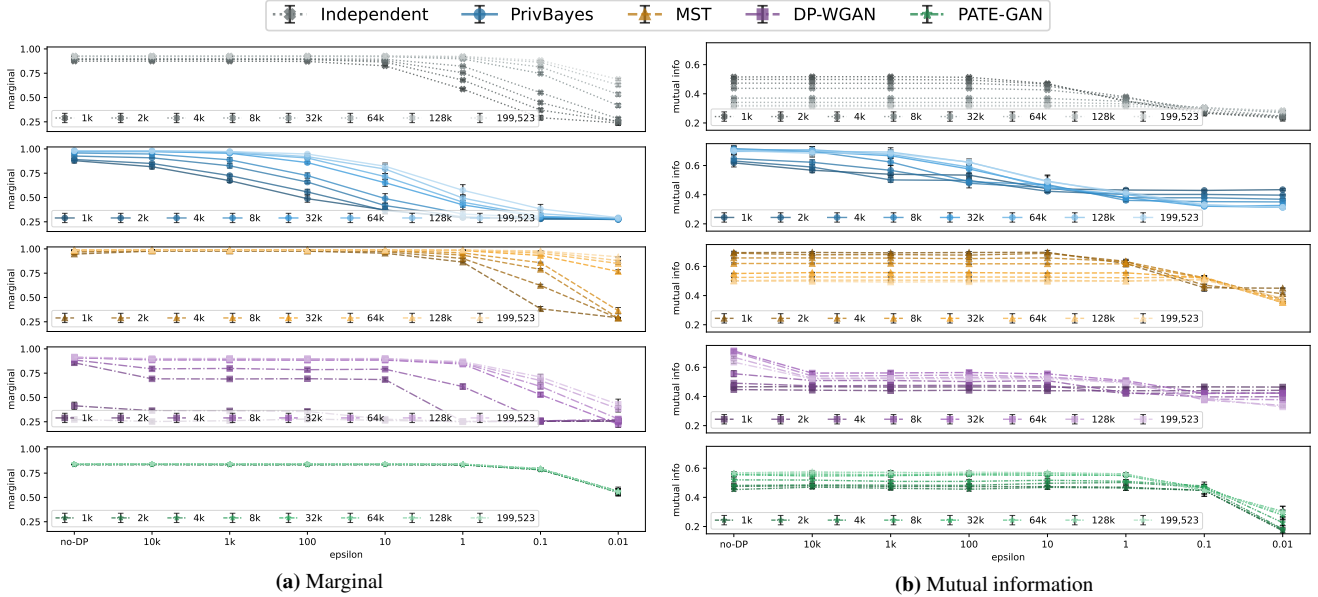


Figure 2: Marginal and pairwise mutual info similarity for different ϵ levels, on *Census*, varying n .

pendent for different levels of ϵ . This demonstrates that both MST and PrivBayes suffer from the curse of dimensionality, which contradicts recent work by Li, Wang, and Cheng [49].

The GANs behave less predictably, and their performance is not monotonic when the dimensions are varied. In all cases, PATE-GAN outperforms DP-WGAN, almost on par with MST for $\epsilon > 0.1$ for *Eye Gauss*. For *Corr Gauss*, however, it cannot capture the off-diagonal correlation sufficiently well, creating data with correlation closer to 0.3 as opposed to 0.5 for the real one. Interestingly, varying the dataset dimensions affects DP-WGAN differently — for both datasets, increasing n yields more correlated distributions with mean around 0, while, for *Corr Gauss*, increasing d (beyond 128) makes the model generate data with relatively un-

correlated columns (≤ 0.2) but with mean further away from 0 (> 0.5). In fact, for *Corr Gauss*, the model cannot distinguish between off-diagonal and other correlations for $d = 32$ and creates data with equal correlation.

4.3 Similarity

In Fig. 2, we plot marginal and pairwise mutual information similarities between the real and synthetic datasets for *Census* with varying n . In Appendix E.3, we also report the metrics for *Covertime* (see Fig. 9) while for *Census*, we show a zoomed-in plot for MST and PATE-GAN (Fig. 10), visualized PrivBayes and MST networks (Fig. 11), and broken down mutual information for connected vs. non-connected nodes (Fig. 12).

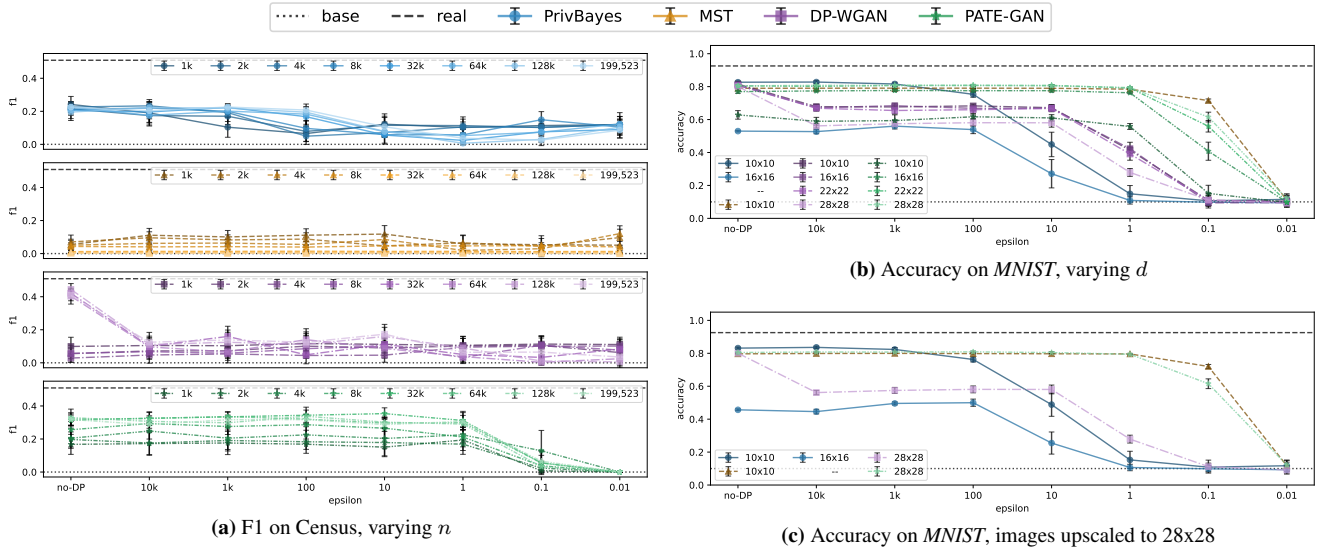


Figure 3: F1 and accuracy for different ϵ levels, on *Census*, varying n and *MNIST*, varying d .

Looking at the marginal similarity for *Census*, Independent, PrivBayes, MST, and DP-WGAN behave as expected, as higher n results in monotonically better scores. The fact that Independent outperforms PrivBayes and the GANs for $\epsilon \leq 10$ should not surprise as it only captures the marginal distributions and does not “waste” any privacy budget for other purposes. With increasing n , there is also an improvement for PATE-GAN, but the sensitivity is much lower. Fig. 10a shows that, when there is only little data available ($n < 4k$), adding some privacy ($10k \leq \epsilon \leq 10$), once again, helps MST.

As for the mutual information similarity (see Fig. 2b, 9b for *Census* and *Covertypes*), adding more data points to the training data yields worse scores for Independent and MST. This is a previously unobserved phenomenon for MST and could be due to the overfitting of the model to its objective function (i.e., all 1-way and 41 2-way marginals as seen in Fig. 11b), thus failing to capture all 2-way marginals. The effect is also visible in Fig. 12, where MST suffers a more significant drop in scores of connected vs. non-connected nodes compared to PrivBayes (which in turn models a much larger number of connections, 120, as seen in Fig. 11a).

For $n > 8k$, PATE-GAN outperforms MST (Fig. 10b) too; this could be explained by its training procedure, which prioritizes creating plausible synthetic data points (i.e., implicitly maintaining correlations between columns). For *Covertypes*, however, PATE-GAN fails to capture the mutual information sufficiently well. Most likely due to the nature of the dataset which is heavily imbalanced and has a multi-class target column, all undesirable conditions for PATE-GAN as observed by [31].

Finally, with PrivBayes and DP-WGAN, increasing n helps the mutual information score for less strict levels of privacy, but only up to $\epsilon = 1$. Whereas for $\epsilon \leq 1$, one would be better off training the models on less data.

4.4 Classification

Finally, we report the F1-score on *Census* with varying n and accuracy on *MNIST* with different resolutions (features) in Fig. 3a and 3b. In Appendix E.5, we present additional results, i.e., accuracy on *Mix Gauss Sup* with varying n , d (Fig. 22), and accuracy/F1 on *Census* and *Connect 4* (Fig. 23, 24).

Looking at *Mix Gauss Sup*, PrivBayes, once again, behaves as expected for different n and d . There is a common trend for MST and DP-WGAN, as both models need at least 16k data points to achieve better than random accuracy. Similarly, if there are too many features, 128 for MST and ≥ 256 for DP-WGAN, the accuracy approaches the random baseline. Varying n does not seem to be a significant factor for PATE-GAN as accuracy tends to be close to the real one for $\epsilon > 0.1$. Increasing d , however, has a negative effect, which is in contrast with previous experiments.

As for *Census*, we consider both accuracy and F1 as the dataset is imbalanced (93.8% of the people make less than \$50k/year). Somewhat unexpectedly, DP-WGAN comes closest to the real F1 baseline but only for the “no-DP” case. Overall, PATE-GAN is the only model with an F1-score consistently close to 0.35, provided that it was trained on at least 8k points. For MST, increasing n helps accuracy (see Fig. 23) but at the expense of F1, meaning that the classifiers trained on the synthetic data overfit to the majority class. This behavior aligns with previous studies on DP generative models trained on imbalanced data [32] even though they have not tested MST explicitly.

We observe very similar trends for *Connect 4* – PATE-GAN is the only model comfortably beating the random baseline and achieving the most consistent F1-score, MST trades higher accuracy for lower F1 with increasing n , while DP-WGAN is the best model for the “no-DP” case.

These trends are very close to the ones observed in the similarity experiments from Sec. 4.3; the relative overper-

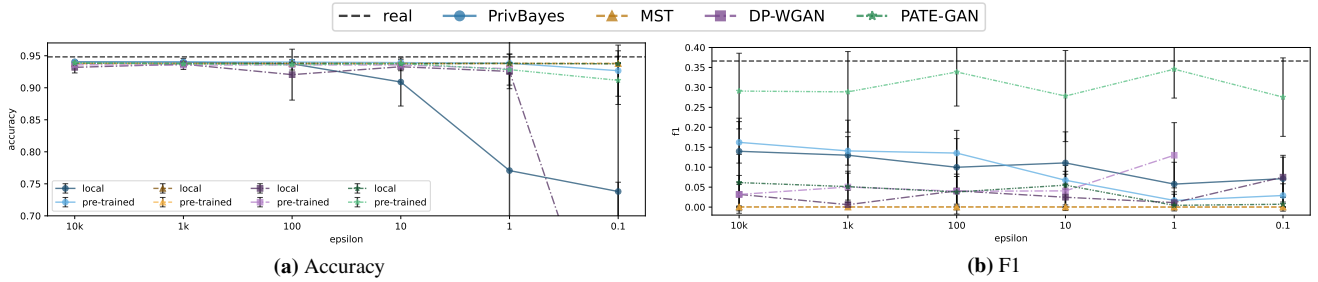


Figure 4: Accuracy and F1 on local data and using a pre-trained model for different ϵ levels, *Census*.

formance of the GAN models compared to MST is in direct contradiction with previous studies [74]. Although we cannot say for sure, we believe that this might, in part, be due to not using the original GAN implementations but relying on third-party ones. Unfortunately, Tao et al. [74] dismiss them as good candidates while arguably overstating the capabilities of other approaches.

As for the accuracy on *MNIST* (Fig. 3b), we see that more features (i.e., images with higher resolution/better quality) deteriorate the performance of PrivBayes and DP-WGAN but help PATE-GAN. In principle, we could expect higher-resolution images to improve both GAN models, but this is the case only for PATE-GAN. However, none of the models approach the real baseline (0.9 accuracy). While this is expected for graphical models, it is somewhat surprising for the GANs. We believe this is because both GANs rely only on feed-forward layers and not CNNs. MST trained on 10x10 images performs very well, achieving 0.8 accuracy, on par with PATE-GAN ($d > 10 \times 10$) for $\epsilon > 0.1$. Again, this might be surprising, as MST does not explicitly model higher-level dependencies, which is important in the image domain.

4.5 Take-Aways

Overall, our experiments shed light on the effects of different generative models, various DP mechanisms, and different dimensions of the training dataset on downstream tasks over the synthetic data. Specifically, we show that the effects are mixed, and no single best-performing model exists.

More training data helps the graphical models but, unexpectedly, could cause MST to overfit and degrade its performance on tasks that require capturing complex relationships (e.g., classification). We also refute claims that MST is scalable (it cannot handle more than 128 columns). Additionally, we show that, in some instances, a small degree of privacy can act as regularization and actually help when presented with a limited amount of data.

The effects of varying the dataset dimensions are more unpredictable (more variable and usually not monotonic) for GANs. While they underperform at simple tasks on controllable datasets, in contrast to previous papers [56, 74], we consistently demonstrate that PATE-GAN could be quite competitive at more challenging tasks and improve with high-dimensional datasets.

Lessons for Practitioners. Overall, our analysis highlights the following actionable recommendations. If the training

data is small ($d \leq 100$) and the downstream task is simple (i.e., capturing statistics/marginals), practitioners would be better off using graphical models. On the other hand, if the dataset is high-dimensional, there are enough records, and the task is more complex (i.e., machine learning-related), GANs are a better choice. In both cases, one could benefit from dataset sampling or early stopping, especially with strict privacy constraints.

5 Discussion and Conclusion

In this paper, we studied and compared how different DP generative models distribute their privacy budget by considering how they scale in terms of increasing dimensions of the dataset, and how these factors affect the quality of the resulting synthetic data for various tasks. We did so to show which models are best suited for different settings and tasks. In the rest of this section, we offer some first-cut solutions and discuss possible future research directions, limitations, and broader impacts.

Increasing Number of Features. Our evaluation showed that increasing the data features results in synthetic data with progressively worse performance on the downstream task (except for PATE-GAN with *MNIST*). Furthermore, the graphical models (which perform better at lower dimensional datasets) cannot scale beyond 128/256 dimensions. A logical follow-up would be to try and reduce the dimensionality of the dataset, train/generate synthetic data in the lower space (this would also help with the DP budget) using the better-suited models, and, if necessary upscale to the original space. Tantipongpipat et al. [73] propose a similar approach, combining VAE and GAN.

As a proof of concept, in Fig. 3c, we downscale *MNIST* images using standard tools to 10x10/16x16, train MST (on 10x10) and PrivBayes (on 10x10 and 16x16), generate synthetic images, and then upscale them back to 28x28. Comparing classifiers trained on both real and synthetic images, we observe that: 1) classifiers trained on MST-generated data perform very well (on par with PATE-GAN trained on the original images), and 2) neither of MST/PrivBayes lose utility compared to when they were tested on downscaled real images (Fig. 3b). Another way to improve on a particular task would be to investigate the most relevant/important features and spend the privacy budget strategically [70]. Alternatively, we could choose the simplest “good enough” model,

e.g., Independent preserved marginal similarity even in high dimensions.

Increasing Number of Rows. We also observed that more data does not always translate to improved quality for all models and evaluations (e.g., the GAN models and MST, apart from marginal similarity). On the other hand, for some models (MST and DP-WGAN), a minimum data threshold is needed to perform better than random. Therefore, more research is needed to find a good balance. One avenue could be to investigate optimal times for early stopping or dataset sampling techniques. Also, one could build relevant public datasets for the tabular domain and develop pre-trained models; researchers and practitioners could then fine-tune the models on their specific (private) dataset [37]. This approach has proved to be very promising in other areas, including NLP [48, 81] and vision [23, 34, 76].

As another proof of concept, in Fig. 4, we report accuracy and F1-scores from classifiers fitted on datasets generated by 1) generative models trained on local data only (n approx. 16k or all individuals with known residence region in *Census*), and 2) “no-DP” pre-trained generative models on a larger amount of data (n approx. 180k) and fine-tuned on the local data. We see that PrivBayes benefits greatly from pre-training, its performance is close to the real data even for $\epsilon = 0.1$. Classifiers trained on MST and PATE-GAN data have satisfactory accuracy but display F1 close to 0. Pre-training on bigger data alleviates this concern for PATE-GAN, in fact, F1 approaches the real baseline. Unfortunately, the effect on MST is negligible. While it is not surprising that pre-training helps GANs, we observe some benefits for graphical models as well (only for PivBayes), but more work needs to be done in this direction.

Limitations. Overall, our work takes an important step in profiling state-of-the-art models for DP synthetic data generation and their use for downstream tasks. However, we only focus on two approaches – graphical and deep generative models as motivated in Sec. 3 – leaving others (e.g., the models presented in Appendix B) to future work. Also, similarly to other studies [74], we use the default hyperparameters for all models, which might not result in optimal performance.

Broader Impacts. While we study generative models with DP guarantees that explicitly minimize privacy concerns, applying DP comes with its own limitations and challenges [21].

For example, generated synthetic data may differ from training data in various ways, causing potential disparity [32] and fairness [3, 68] issues by propagating or even exacerbating the historical biases.

References

- [1] M. Abadi, A. Chu, I. Goodfellow, H. B. McMahan, I. Mironov, K. Talwar, and L. Zhang. Deep learning with differential privacy. In *ACM CCS*, 2016.
- [2] N. C. Abay, Y. Zhou, M. Kantarcioglu, B. Thuraisingham, and L. Sweeney. Privacy preserving synthetic data release using deep learning. In *ECML PKDD*, 2018.
- [3] M. Abroshan, M. M. Khalili, and A. Elliott. Counterfactual Fairness in Synthetic Data Generation. In *SyntheticData4ML*, 2022.
- [4] Accelario. Realistic test data in minutes. <https://accelario.com/products/synthetic-data/>, 2023.
- [5] G. Acs, L. Melis, C. Castelluccia, and E. De Cristofaro. Differentially private mixture of generative neural networks. *IEEE TKDE*, 2018.
- [6] M. Alzantot and M. Srivastava. Differential Privacy Synthetic Data Generation using WGANs. <https://github.com/nsl/nist-differential-privacy-synthetic-data-challenge>, 2019.
- [7] D. S. Antonova. Practical differential privacy in high dimensions. <https://era.ed.ac.uk/handle/1842/20405>, 2016.
- [8] M. Arjovsky, S. Chintala, and L. Bottou. Wasserstein generative adversarial networks. In *ICML*, 2017.
- [9] C. Arnold and M. Neunhoffer. Really Useful Synthetic Data—A Framework to Evaluate the Quality of Differentially Private Synthetic Data. *arXiv:2004.07740*, 2020.
- [10] H. J. Asghar, M. Ding, T. Rakotoarivelo, S. Mrabet, and D. Kaafar. Differentially Private Release of Datasets using Gaussian Copula. *JPC*, 2021.
- [11] S. Aydoore, W. Brown, M. Kearns, K. Kenthapadi, L. Melis, A. Roth, and A. A. Siva. Differentially private query release through adaptive projection. In *ICML*, 2021.
- [12] B. Balle, G. Cherubin, and J. Hayes. Reconstructing Training Data with Informed Adversaries. In *IEEE S&P*, 2022.
- [13] M. I. Belghazi, A. Baratin, S. Rajeshwar, S. Ozair, Y. Bengio, A. Courville, and D. Hjelm. Mutual information neural estimation. In *ICML*, 2018.
- [14] G. Benedetto, J. C. Stanley, E. Totty, et al. The creation and use of the SIPP synthetic Beta v7. 0. *US Census Bureau*, 2018.
- [15] M. Boedihardjo, T. Strohmer, and R. Vershynin. Covariance’s Loss is Privacy’s Gain: Computationally Efficient, Private and Accurate Synthetic Data. *arXiv:2107.05824*, 2021.
- [16] K. Cai, X. Lei, J. Wei, and X. Xiao. Data synthesis via differentially private markov random fields. *PVLDB*, 2021.
- [17] N. Carlini, C. Liu, Ú. Erlingsson, J. Kos, and D. Song. The secret sharer: Evaluating and testing unintended memorization in neural networks. In *USENIX Security*, 2019.
- [18] T. Chanyaswad, C. Liu, and P. Mittal. Ron-gauss: Enhancing utility in non-interactive private data release. *PoPETs*, 2019.
- [19] K. Chaudhuri, C. Monteleoni, and A. D. Sarwate. Differentially private empirical risk minimization. *JMLR*, 2011.
- [20] D. Chen, N. Yu, Y. Zhang, and M. Fritz. Gan-leaks: A taxonomy of membership inference attacks against generative models. In *ACM CCS*, 2020.
- [21] R. Cummings, D. Desfontaines, D. Evans, R. Geambasu, M. Jagielski, Y. Huang, P. Kairouz, G. Kamath, S. Oh, O. Ohrimenko, N. Papernot, R. Rogers, M. Shen, S. Song, W. Su, A. Terzis, A. Thakurta, S. Vassilvitskii, Y.-X. Wang, L. Xiong, S. Yekhanin, D. Yu, H. Zhan, and W. Zhang. Challenges towards the Next Frontier in Privacy. *arXiv:2304.06929*, 2023.
- [22] Datagen. Guide: Synthetic Data. <https://datagen.tech/guides/synthetic-data/synthetic-data/>, 2023.
- [23] S. De, L. Berrada, J. Hayes, S. L. Smith, and B. Balle. Unlocking high-accuracy differentially private image classification through scale. *arXiv:2204.13650*, 2022.
- [24] D. Dua and C. Graff. UCI Machine Learning Repository. <http://archive.ics.uci.edu/ml>, 2017.

- [25] C. Dwork, K. Kenthapadi, F. McSherry, I. Mironov, and M. Naor. Our data, ourselves: Privacy via distributed noise generation. In *EuroCrypt*, 2006.
- [26] C. Dwork, F. McSherry, K. Nissim, and A. Smith. Calibrating noise to sensitivity in private data analysis. In *TCC*, 2006.
- [27] C. Dwork, M. Naor, O. Reingold, G. N. Rothblum, and S. Vadhan. On the complexity of differentially private data release: efficient algorithms and hardness results. In *ACM STOC*, 2009.
- [28] C. Dwork, A. Roth, et al. The algorithmic foundations of differential privacy. *Foundations and Trends in Theoretical Computer Science*, 2014.
- [29] L. Frigerio, A. S. de Oliveira, L. Gomez, and P. Duverger. Differentially private generative adversarial networks for time series, continuous, and discrete open data. In *IFIP SEC*, 2019.
- [30] S. Gambs, F. Ladouceur, A. Laurent, and A. Roy-Gaumond. Growing synthetic data through differentially-private vine copulas. *PoPETS*, 2021.
- [31] G. Ganev. DP-SGD vs PATE: Which Has Less Disparate Impact on GANs? *PPAI*, 2022.
- [32] G. Ganev, B. Oprisanu, and E. De Cristofaro. Robin Hood and Matthew Effects: Differential Privacy Has Disparate Impact on Synthetic Data. In *ICML*, 2022.
- [33] C. Ge, S. Mohapatra, X. He, and I. F. Ilyas. Kamino: Constraint-Aware Differentially Private Data Synthesis. *PVLDB*, 2021.
- [34] A. Golatkar, A. Achille, Y.-X. Wang, A. Roth, M. Kearns, and S. Soatto. Mixed Differential Privacy in Computer Vision. In *CVPR*, 2022.
- [35] Gretel. Gretel Synthetics. <https://gretel.ai/synthetics>, 2023.
- [36] C. Guo, A. Sablayrolles, and M. Sanjabi. Analyzing Privacy Leakage in Machine Learning via Multiple Hypothesis Testing: A Lesson From Fano. In *ICML*, 2023.
- [37] F. Harder, M. J. Asadabadi, D. J. Sutherland, and M. Park. Differentially Private Data Generation Needs Better Features. *arXiv:2205.12900*, 2022.
- [38] M. Hay, A. Machanavajjhala, G. Miklau, Y. Chen, and D. Zhang. Principled evaluation of differentially private algorithms using dpbench. In *SIGMOD*, 2016.
- [39] J. Hayes, S. Mahloujifar, and B. Balle. Bounding Training Data Reconstruction in DP-SGD. *arXiv:2302.07225*, 2023.
- [40] J. Hayes, L. Melis, G. Danezis, and E. De Cristofaro. Logan: Membership inference attacks against generative models. In *PoPETS*, 2019.
- [41] B. Hilprecht, M. Härterich, and D. Bernau. Monte Carlo and Reconstruction Membership Inference Attacks against Generative Models. In *PoPETS*, 2019.
- [42] ICO UK. Chapter 5: Privacy-enhancing technologies (PETs). <https://ico.org.uk/media/about-the-ico/consultations/4021464/chapter-5-anonymisation-pets.pdf>, 2022.
- [43] J. Jordon, L. Szpruch, F. Houssiau, M. Bottarelli, G. Cherubin, C. Maple, S. N. Cohen, and A. Weller. Synthetic Data—what, why and how? *arXiv:2205.03257*, 2022.
- [44] J. Jordon, J. Yoon, and M. Van Der Schaar. PATE-GAN: Generating synthetic data with differential privacy guarantees. In *ICLR*, 2018.
- [45] Y. LeCun, C. Cortes, and C. Burges. MNIST handwritten digit database. *ATT Labs*, 2010.
- [46] D. Li, Y. Cao, and Y. Yao. Optimizing Random Mixup with Gaussian Differential Privacy. *arXiv:2202.06467*, 2022.
- [47] H. Li, L. Xiong, and X. Jiang. Differentially private synthesis of multi-dimensional data using copula functions. In *EDBT*, 2014.
- [48] X. Li, F. Tramer, P. Liang, and T. Hashimoto. Large language models can be strong differentially private learners. *ICLR*, 2022.
- [49] X. Li, C. Wang, and G. Cheng. Statistical Theory of Differentially Private Marginal-based Data Synthesis Algorithms. In *ICLR*, 2023.
- [50] T. Liu, G. Vietri, and S. Z. Wu. Iterative methods for private synthetic data: Unifying framework and new methods. *NeurIPS*, 2021.
- [51] Y. Long, B. Wang, Z. Yang, B. Kailkhura, A. Zhang, C. A. Gunter, and B. Li. G-PATE: Scalable differentially private data generator via private aggregation of teacher discriminators. In *NeurIPS*, 2021.
- [52] S. Mahiou, K. Xu, and G. Ganev. dpart: Differentially Private Autoregressive Tabular, a General Framework for Synthetic Data Generation. *TPDP*, 2022.
- [53] R. McKenna and T. Liu. A simple recipe for private synthetic data generation. <https://differentialprivacy.org/synth-data-1/>, 2022.
- [54] R. McKenna, G. Miklau, M. Hay, and A. Machanavajjhala. HDMM: Optimizing error of high-dimensional statistical queries under differential privacy. *arXiv:2106.12118*, 2021.
- [55] R. McKenna, G. Miklau, and D. Sheldon. Winning the NIST Contest: A scalable and general approach to differentially private synthetic data. *JPC*, 2021.
- [56] R. McKenna, B. Mullins, D. Sheldon, and G. Miklau. Aim: An adaptive and iterative mechanism for differentially private synthetic data. *PVLDB*, 2022.
- [57] R. McKenna, D. Sheldon, and G. Miklau. Graphical-model based estimation and inference for differential privacy. In *ICML*, 2019.
- [58] F. McSherry and K. Talwar. Mechanism design via differential privacy. In *FOCS*, 2007.
- [59] J. P. Near and C. Abuah. Programming Differential Privacy. <https://uvm-plaid.github.io/programming-dp>, 2021.
- [60] NHS England. A&E Synthetic Data. <https://data.england.nhs.uk/dataset/a-e-synthetic-data>, 2021.
- [61] NIST. 2018 Differential Privacy Synthetic Data Challenge. <https://www.nist.gov/ctl/pscr/open-innovation-prize-challenges/past-prize-challenges/2018-differential-privacy-synthetic>, 2018.
- [62] NIST. 2018 The Unlinkable Data Challenge. <https://www.nist.gov/ctl/pscr/open-innovation-prize-challenges/past-prize-challenges/2018-unlinkable-data-challenge>, 2018.
- [63] NIST. 2020 Differential Privacy Temporal Map Challenge. <https://www.nist.gov/ctl/pscr/open-innovation-prize-challenges/past-prize-challenges/2020-differential-privacy-temporal>, 2020.
- [64] N. Papernot, M. Abadi, U. Erlingsson, I. Goodfellow, and K. Talwar. Semi-supervised knowledge transfer for deep learning from private training data. In *ICLR*, 2017.
- [65] N. Papernot, S. Song, I. Mironov, A. Raghunathan, K. Talwar, and Ú. Erlingsson. Scalable private learning with pate. In *ICLR*, 2018.
- [66] A. Pearce. Can a Model Be Differentially Private and Fair? <https://pair.withgoogle.com/explorables/private-and-fair>, 2022.
- [67] B. Poole, S. Ozair, A. Van Den Oord, A. Alemi, and G. Tucker. On variational bounds of mutual information. In *ICML*, 2019.
- [68] D. Pujol, A. Gilad, and A. Machanavajjhala. PreFair: Privately Generating Justifiably Fair Synthetic Data. *PVLDB*, 2022.

- [69] B. Rhodes, K. Xu, and M. U. Gutmann. Telescoping density-ratio estimation. *NeurIPS*, 2020.
- [70] L. Rosenblatt, J. Allen, and J. Stoyanovich. Spending Privacy Budget Fairly and Wisely. *arXiv:2204.12903*, 2022.
- [71] Syntho. AI-generated Synthetic Data, easy and fast access to high quality data? <https://www.syntho.ai/ai-generated-synthetic-data-easy-and-fast-access-to-high-quality-data/>, 2023.
- [72] S. Takagi, T. Takahashi, Y. Cao, and M. Yoshikawa. P3gm: Private high-dimensional data release via privacy preserving phased generative model. In *IEEE ICDE*, 2021.
- [73] U. Tantipongpipat, C. Waites, D. Boob, A. Siva, and R. Cummings. Differentially private mixed-type data generation for unsupervised learning. In *IISA*, 2021.
- [74] Y. Tao, R. McKenna, M. Hay, A. Machanavajjhala, and G. Miklau. Benchmarking differentially private synthetic data generation algorithms. *PPAI*, 2022.
- [75] TechCrunch. The market for synthetic data is bigger than you think. <https://techcrunch.com/2022/05/10/the-market-for-synthetic-data-is-bigger-than-you-think/>, 2022.
- [76] F. Tramer and D. Boneh. Differentially private learning needs better features (or much more data). *ICLR*, 2021.
- [77] J. Ullman and S. Vadhan. PCPs and the hardness of generating private synthetic data. In *TCC*, 2011.
- [78] G. Vietri, G. Tian, M. Bun, T. Steinke, and S. Wu. New oracle-efficient algorithms for private synthetic data release. In *ICML*, 2020.
- [79] R. Webster, J. Rabin, L. Simon, and F. Jurie. Detecting overfitting of deep generative networks via latent recovery. In *IEEE CVPR*, 2019.
- [80] L. Xie, K. Lin, S. Wang, F. Wang, and J. Zhou. Differentially private generative adversarial network. *arXiv:1802.06739*, 2018.
- [81] D. Yu, S. Naik, A. Backurs, S. Gopi, H. A. Inan, G. Kamath, J. Kulkarni, Y. T. Lee, A. Manoel, L. Wutschitz, et al. Differentially private fine-tuning of language models. *ICLR*, 2022.
- [82] J. Zhang, G. Cormode, C. M. Procopiuc, D. Srivastava, and X. Xiao. PrivBayes: Private data release via bayesian networks. *ACM TODS*, 2017.
- [83] W. Zhang, J. Zhao, F. Wei, and Y. Chen. Differentially private high-dimensional data publication via Markov network. *EAI Endorsed Transactions on Security and Safety*, 2019.
- [84] X. Zhang, S. Ji, and T. Wang. Differentially private releasing via deep generative model (technical report). *arXiv:1801.01594*, 2018.
- [85] Z. Zhang, T. Wang, J. Honorio, N. Li, M. Backes, S. He, J. Chen, and Y. Zhang. PrivSyn: Differentially Private Data Synthesis. In *USENIX Security*, 2021.

A Additional Background and Related Work

Differential Privacy (DP). A randomized algorithm \mathcal{A} satisfies (ϵ, δ) -DP if, for all of its possible outputs S , and all neighboring datasets D and D' (D and D' are identical except for a single data row), the following holds [26, 28]:

$$P[\mathcal{A}(D) \in S] \leq \exp(\epsilon) \cdot P[\mathcal{A}(D') \in S] + \delta \quad (1)$$

Here, ϵ is a positive, real number (also referred to as the *privacy budget*) that quantifies the information leakage, while

δ , usually a very small real number, allows for a probability of failure. In other words, looking at the output of the computation (e.g., the trained model), it is impossible to distinguish whether any individual’s data was included in the input dataset.

In our evaluation, we study generative models relying on a variety of well-known DP techniques: the Laplace [26], Exponential [25], and Gaussian mechanisms [58], Differentially Private Stochastic Gradient Descent (DP-SGD) [1], and Private Aggregation of Teacher Ensembles (PATE) [64, 65].

Due to its composition and robustness to post-processing properties, DP allows different DP mechanisms to be combined while the overall privacy budget is tracked and DP-trained models to be re-used without further privacy leakage.

Synthetic Data. In this paper, we focus on techniques to create synthetic data through generative machine learning models. A sample dataset D^n , consisting of n iid drawn records with d features from the population $D^n \sim P(\mathbb{D})$, is fed as input to the generative model training algorithm $GM(D^n)$ during the fitting step. In turn, $GM(D^n)$ updates its internal parameters θ to learn $P_{\theta}(D^n)$, (a lower-dimensional) representation of the probability of the sample dataset $P(D^n)$, and outputs the trained model $\overline{GM}(D^n)$. Then, $\overline{GM}(D^n)$ could be sampled to generate a synthetic data of size n' , $S^{n'} \sim P_{\theta}(D^n)$. Since both the fitting and generation steps are stochastic, one can train the generative model m times and sample s synthetic datasets for each trained model to get confidence intervals.

B DP Generative Models

There is a vast literature of DP techniques for tabular synthetic data generation, namely, copulas [10, 30, 47], graphical models [16, 52, 55, 82, 83], workload/query based [11, 50, 78], Variational Autoencoders (VAEs) [2, 5, 72], Generative Adversarial Networks (GANs) [6, 29, 44, 51, 73, 80, 84], and other approaches [18, 33, 85].

Next, we describe the models used in our evaluation as motivated in Sec. 3. The specific implementations we use are given in footnotes. (Note that we independently implemented Independent and PrivBayes.) For all experiments, the default hyperparameters are used unless stated otherwise.

Independent. As a baseline, we use a simple model that, for all columns, independently captures noisy marginal counts through the Laplace mechanism and then samples from them to generate synthetic data. Though very simple, it has proven to perform better than far more sophisticated models in certain settings [74].

PrivBayes [82] first constructs an optimal Bayesian network by randomly picking up a node (column of the dataset) as the root and iteratively adding one node at a time, maximizing the mutual information between the existing “parent” nodes and a candidate “child” node. Half of ϵ is spent at this step using the Exponential mechanism, while the network degree argument determines the maximum number of parents a given node can have. Then, PrivBayes estimates the result-

ing low-dimensional conditional distributions through computing noisy contingency tables (utilizing the Laplace mechanism) before normalizing and converting them to distributions. Since the network is built iteratively and all computed distributions are conditional, they are also consistent. We run PrivBayes for datasets with columns up to 256, setting the network degree to the default 3 for datasets with fewer than 100 columns and to 2 otherwise.

MST [55]² follows a similar procedure. For selection, it starts with all 1-way marginals and finds attribute pairs (2-way marginals) that form a maximum spanning tree of the underlying correlation graph. This is achieved through first estimating all 2-way marginals using Private-PGM [57] (a post-processing method that infers a data distribution given noisy measurements) and, then, one by one, noisily adding a highly weighted edge to the graph. The edge weights are measured by the L_1 distance between real and estimated 2-way marginals. All selected marginals are measured privately using the Gaussian mechanism. MST allocates 1/3 of the privacy budget to selection and the remaining 2/3 to measurement. We train MST on datasets with up to 128 columns and set $\delta = 10^{-5}$ (to be consistent with DP-WGAN and PATE-GAN).

DP-WGAN [6]³ utilizes the Wasserstein GAN (WGAN) architecture [8], which achieves better learning stability and improves mode collapse issues compared to the original GAN by using Wasserstein distance rather than Jensen-Shannon divergence. The model relies on DP-SGD to ensure the privacy of the discriminator during training, which in turn guarantees the privacy of the generator since it is never exposed to the real data.

PATE-GAN [44]⁴ adapts the PATE framework and combines it with a GAN architecture. The architecture consists of a single generator, t teacher-discriminators, and a student-discriminator. The teacher-discriminators are only presented with disjoint subsets of the training data and are trained to improve their loss with respect to the generator (i.e., classifying samples as real or fake). In contrast, the student-discriminator is trained on noisily aggregated labels provided by the teachers, and its loss gradients are sent to train the generator.

C Datasets

Gaussians. We create four progressively more complex datasets based on the gaussian distribution:

- *Eye Gauss* consists of columns that are independently distributed standard normals.
- *Corr Gauss* (inspired by [13, 67, 69]) is a multivariate normal with mean 0 and covariance matrix with 1s on the diagonal (unit variance), 0.5s on the off-diagonal

(all neighboring columns have correlation 0.5), and 0s everywhere else (not neighboring columns are uncorrelated). The idea is to see if the model would be able to capture the correlation correctly.

- The first two columns of *Mix Gauss Unsup* (inspired by [29]) are a mixture of six gaussians distributed in a ring with center 0, while the remaining columns represent noise in the form of uncorrelated gaussians with mean 0. The model should be able to separate signal from noise and reproduce the six clusters.
- The *Mix Gauss Sup* dataset is the same as the previous one but with an added target column, labeling the six gaussians in a non-linearly separable way. Classifiers trained on the real and on the synthetic data should have similar performance.

For all datasets, we vary the number of columns in the range {8, 16, 32, 64, 128, 256, 512, 1,024} while keeping the rows to 16k. We also vary the number of rows in the range {250, 500, 1k, 2k, 4k, 8k, 16k, 32k, 64k, 128k} while fixing the columns to 32. When applicable, we create test datasets with size equal to 20% of the training.

Covertime. The Covertime dataset [24] contains cartographic variables such as wilderness areas and soil types. There are 55 variables (10 numerical and 45 categorical), including the target consisting of seven distinct forest cover types. While there are 581,012 data points, we separate 20% (116,203) for testing purposes and vary the training points in the range {1k, 2k, 4k, 8k, 16k, 32k, 64k, 128k, 256k, 464,809}.

Census. The Census dataset [24] is extracted from the 1994 and 1995 Current Population Surveys conducted by the US Census Bureau. It contains 41 (six numerical and 35 categorical) demographic and employment-related variables. The target column indicates whether the individual’s income exceeds \$50k/year. The dataset consists of 199,523 training and 99,762 testing instances. We vary the training points in the range {1k, 2k, 4k, 8k, 16k, 32k, 64k, 128k, 199,523} (the latter being the original size).

Connect 4. The Connect 4 dataset [24] contains all legal positions in the game of connect-4 (vertically, horizontally, or diagonally) in which neither player has won yet and the next move is not forced. The outcome class is the game theoretical value for the first player. The datasets consists of 67,557 data instances and 43 categorical features, including the target class. We set aside 20% (13,512) of the data for testing and vary the training size in the range {1k, 2k, 4k, 8k, 16k, 32k, 54,045}.

MNIST. The MNIST dataset [45] is a collection of greyscale handwritten digits. There are 60k training and 10k testing samples. The task is to classify the digit. We experiment with a varying number of features. On top of the original 28x28 pixels, we also rescale the images to 10x10, 16x16, and 22x22.

²<https://github.com/ryan112358/private-pgm>

³https://github.com/nesl/nist_differential_privacy_synthetic_data_challenge

⁴<https://bitbucket.org/mvdschaar/mlforhealthlabpub>

D Downstream Tasks

We outline the downstream tasks and metrics used in our evaluation. As mentioned in Sec. 4, all reported metrics are averaged over 25 synthetic datasets.

Scalability. We measure run time (in minutes) for both training and generation steps.

Statistics. We report the mean as well as pairwise correlation averaged across all columns/pairs of columns. Furthermore, sometimes we distinguish between off-diagonal and other (excluding the diagonal and off-diagonal) correlation.

Similarity. We evaluate 1-way marginal similarity as well as pairwise mutual information similarity. Both of these metrics are averaged across all columns, too. We uniformly discretize the columns to 20 bins before calculating the metrics.

PCA and Clustering. We fit PCA to the high-dimensional datasets and visualize the KDE on the first two components. Furthermore, we fit a Mixture of Gaussians models on the reduced real and synthetic datasets, test on set aside test data, and report silhouette scores.

Classification. We fit logistic regression on the real and synthetic datasets and report accuracy and F1-scores on the unseen test data (neither by the generative model nor the classifier). We limit our evaluation to logistic regression in order to avoid another source of randomness.

E Additional Results and Plots

E.1 Scalability

We report summaries of the run time of the fitting step for *Corr Gauss* with varying n in Table 4 and generation step with varying n and d in Table 5, 6. The results are discussed in Sec. 4.1.

E.2 Statistics

We visualize the average statistics for *Eye Gauss* and *Corr Gauss* with varying dimensions; more precisely, mean and correlation for the former in Fig. 5, 6 and mean and correlation for the latter in Fig. 7, 8. The results are discussed in detail in Sec. 4.2.

E.3 Similarity

Marginal and pairwise mutual information similarity results for all models with varying n on *Covertime* are displayed in Fig. 9 while we plot the zoomed-in metrics for MST and PATE-GAN on *Census* in Fig. 10. We also visualize fitted

networks for MST and PrivBayes in Fig. 11 and break down the mutual information similarly between connected and non-connected nodes in Fig. 12. These experiments are discussed in Sec. 4.3.

E.4 PCA and Clustering

We now focus on Principal Component Analysis (PCA) and clustering tasks.

The Kernel Density Estimation (KDE) on the first 2 PCA components of all four *Gauss* datasets with varying dimensions are plotted in Fig. 14, 15, 16, 17, 18, 19, 20, and 21 while the silhouette scores of clusters predicted by Mixture of Gaussians models fitted to the first 2 PCA components on *Corr Gauss* are shown in Fig. 13.

Analyzing the PCA plots, no models manages to replicate all datasets sufficiently well. PrivBayes probably comes closest for $\epsilon \geq 10$, and for the *Mix Gauss* datasets, it is the only model that properly separates the first two columns creating the six clusters from the rest containing noise. When a tighter privacy budget is applied, or the dataset dimensions are increased, the variance of the synthetic data increases, too, for all datasets. While MST performs very well for *Eye* and *Corr Gauss*, it ultimately fails for the other two as it generates some difficult-to-define structure, probably due to mode collapse. Unsurprisingly, Independent cannot capture *Mix Gauss* distributions either. Unfortunately, the GAN models do not perform well on these datasets either. At the very least, they capture the range of the data well. However, n and d do not seem to be important factors. For $d \geq 32$ and $\epsilon > 0.1$, PATE-GAN generates data that loosely resembles the real, but it is shaped more as a box rather than a ring.

The silhouette scores in Fig. 13 look very variably and noisy, most likely because the clustering was done on the first 2 PCA components instead of the complete datasets due to computational time restrictions. Broadly speaking, they confirm what we observed in the PCA plots. PrivBayes performs very well for $n > 1k$. Varying n strongly affects MST and makes the scores very noisy and unpredictable. PATE-GAN achieves good silhouette scores, greater or equal to 0.45 for all n .

E.5 Classification

The average accuracy for *Mix Gauss Sup* with varying dimensions is plotted in Fig. 22 while the average accuracy and F1 for *Census* and *Connect 4* with increasing n are displayed in Fig. 23, 24. We look at these plots in detail in Sec. 4.4.

DP Model	$n \rightarrow 250$	500	1k	4k	16k	32k	64k	128k
Independent	0.01	0.01	0.01	0.01	0.01	0.02	0.03	0.05
PrivBayes	0.02	0.03	0.03	0.05	0.06	0.07	0.10	0.13
MST	3.23	3.27	3.27	3.28	3.23	3.23	3.32	3.30
DP-WGAN	0.11	0.11	0.13	0.24	0.76	1.42	2.73	5.37
PATE-GAN	0.02	0.03	0.05	0.18	0.76	1.75	4.55	13.40

Table 4: Run time (in minutes) of the model’s fitting step for DP generative models, on *Corr Gauss*, varying n and $d = 32$.

DP Model	$n \rightarrow 250$	500	1k	4k	16k	32k	64k	128k
Independent	0.00	0.00	0.00	0.00	0.01	0.01	0.03	0.06
PrivBayes	0.00	0.00	0.00	0.00	0.01	0.01	0.03	0.05
MST	0.01	0.01	0.01	0.01	0.02	0.02	0.04	0.07
DP-WGAN	0.00	0.00	0.00	0.00	0.01	0.01	0.02	0.04
PATE-GAN	0.00	0.00	0.00	0.00	0.00	0.00	0.00	0.01

Table 5: Run time (in minutes) of the model’s generation step for fitted DP generative models, on *Corr Gauss*, varying n and $d = 32$.

DP Model	$d \rightarrow 8$	16	32	64	128	256	512	1,024
Independent	0.00	0.00	0.01	0.02	0.07	0.24	0.99	3.69
PrivBayes	0.00	0.00	0.01	0.02	0.03	0.07		
MST	0.00	0.01	0.02	0.05	0.13			
DP-WGAN	0.00	0.00	0.01	0.01	0.02	0.06	0.39	1.63
PATE-GAN	0.00	0.00	0.00	0.00	0.01	0.05	0.3	1.57

Table 6: Run time (in minutes) of the model’s generation step for fitted DP generative models, on *Corr Gauss*, varying d and $n = 16k$.

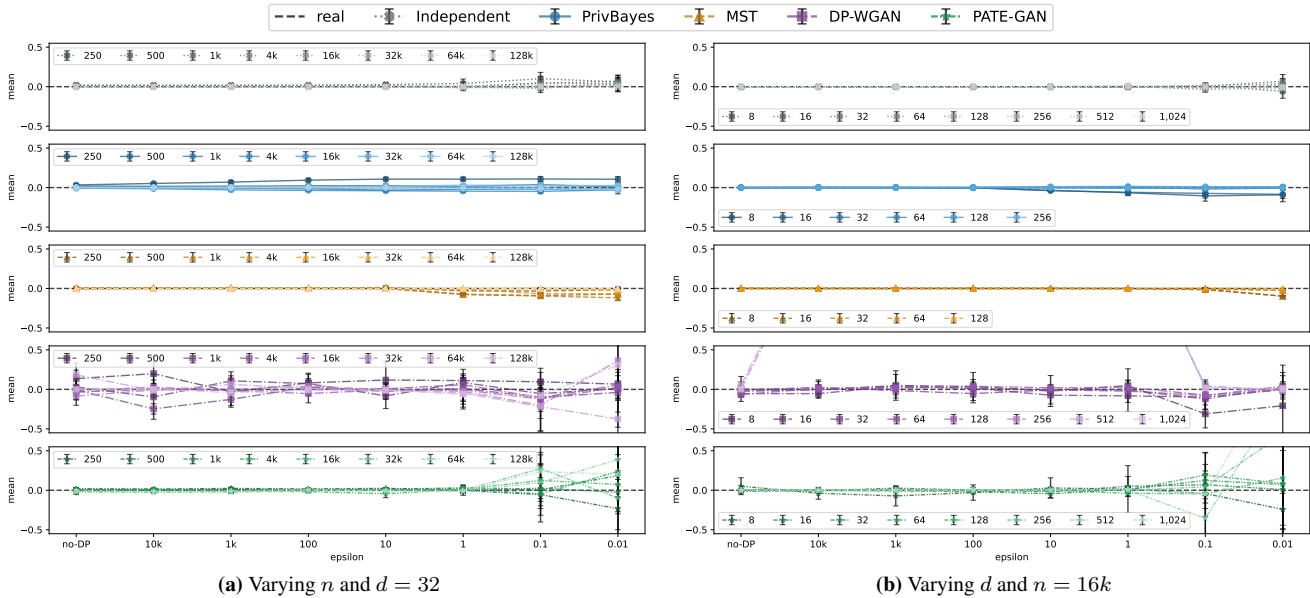


Figure 5: Marginal mean for different ϵ levels, on *Eye Gauss*, varying n and d .

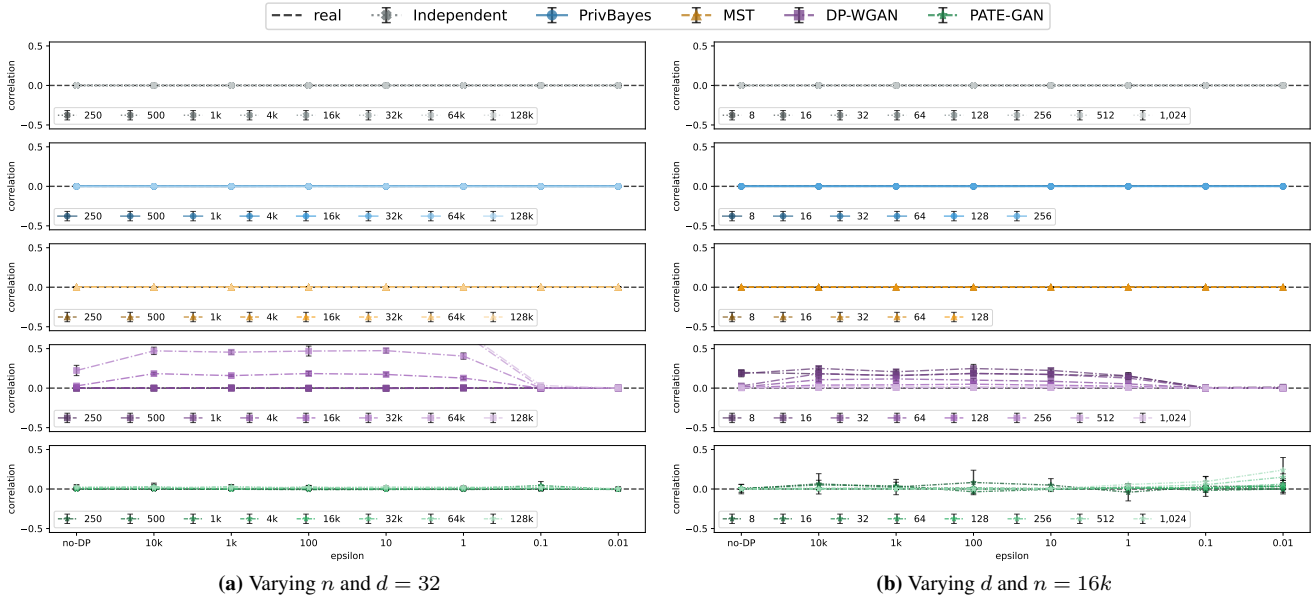


Figure 6: Other (apart from diagonal) pairwise correlation for different ϵ levels, on *Eye Gauss*, varying n and d .

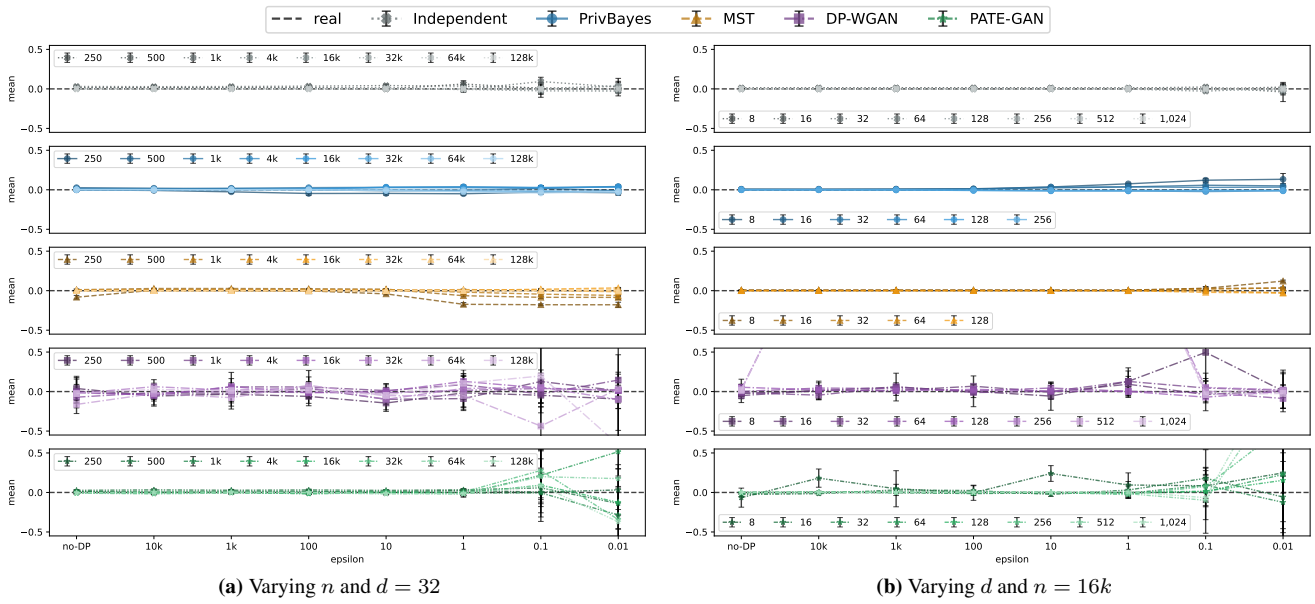


Figure 7: Marginal mean for different ϵ levels, on *Corr Gauss*, varying n and d .

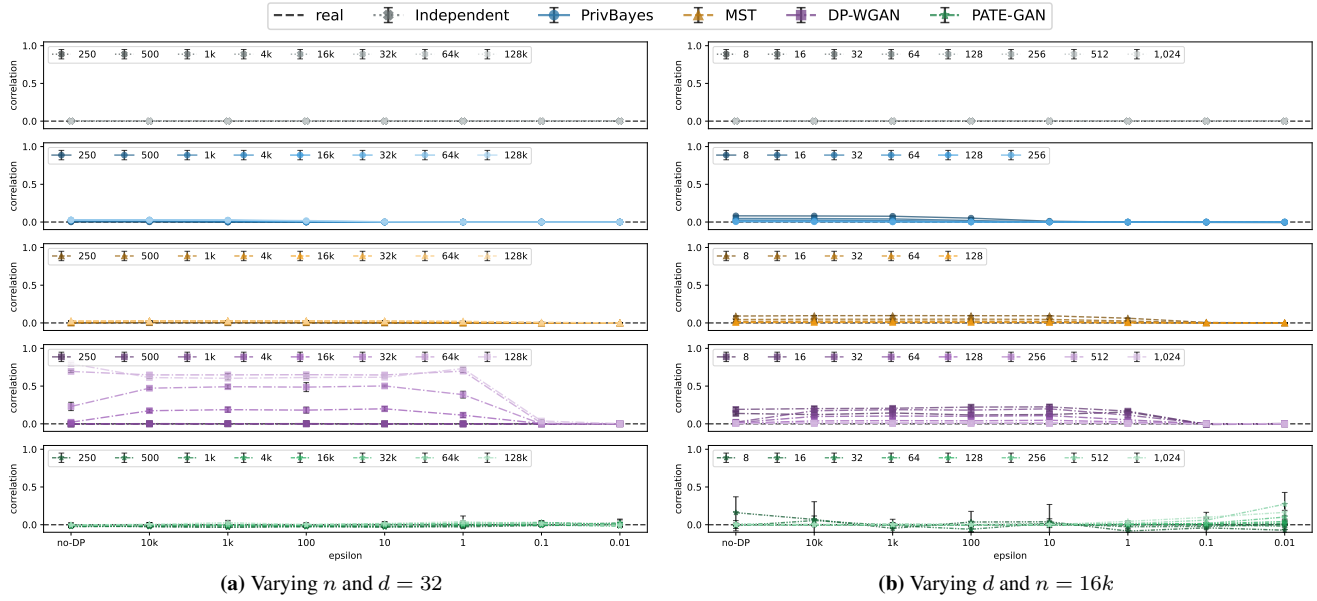


Figure 8: Other (apart from diagonal and off-diagonal) pairwise correlation for different ϵ levels, on *Corr Gauss*, varying n and d .

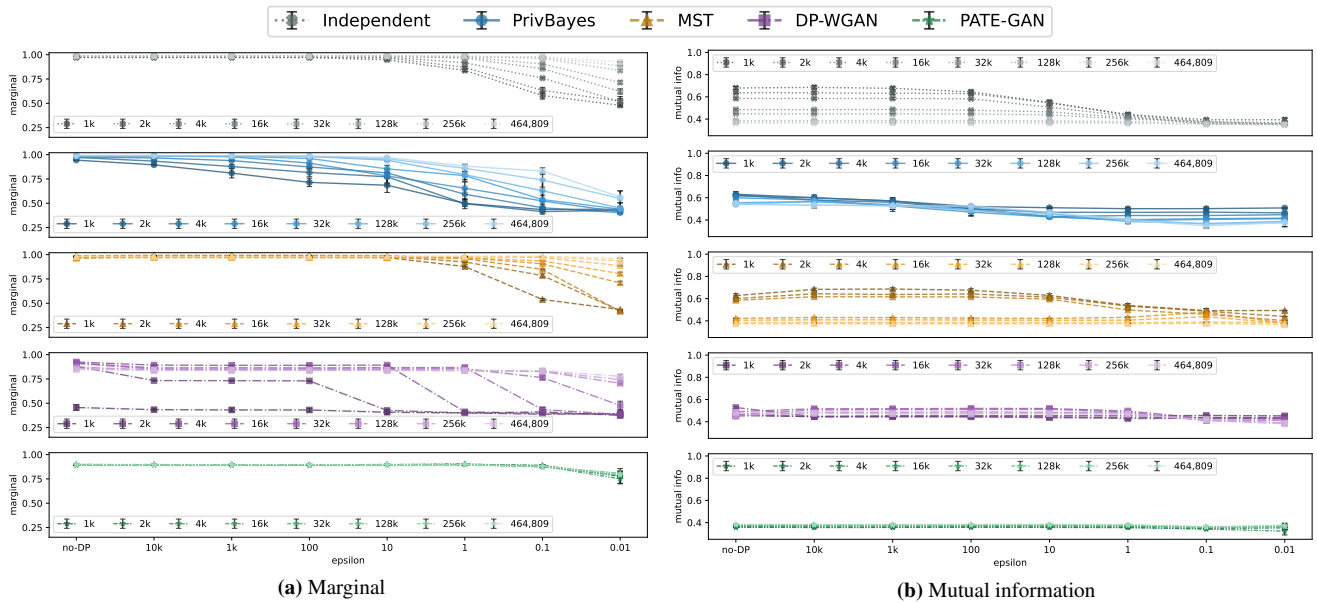


Figure 9: Marginal and pairwise mutual info similarity for different ϵ levels, on *Covertypes*, varying n .

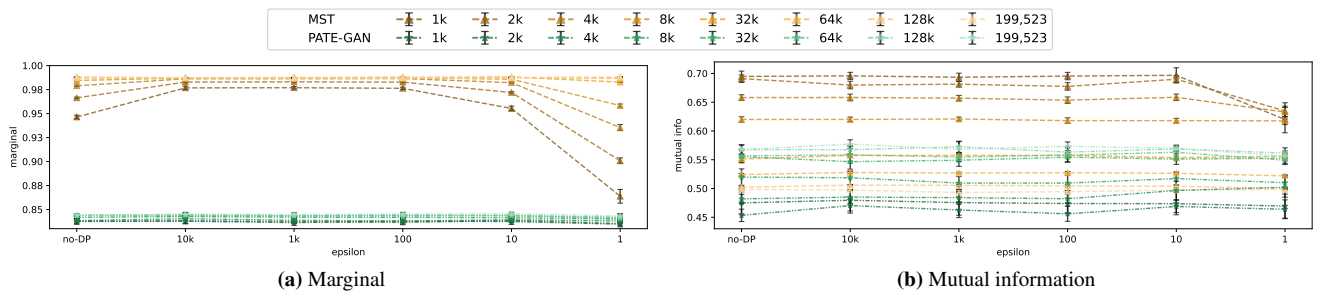
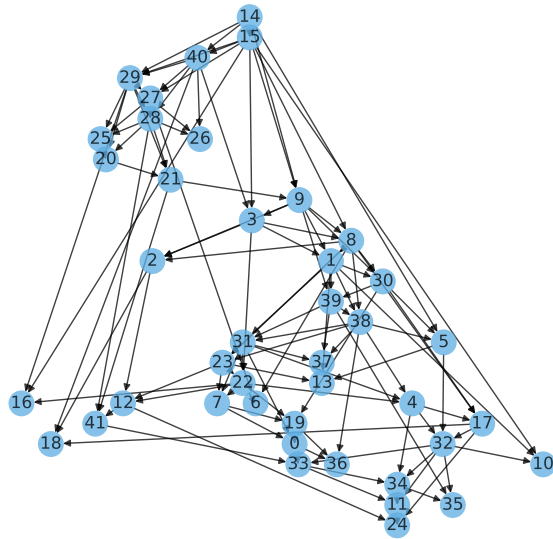
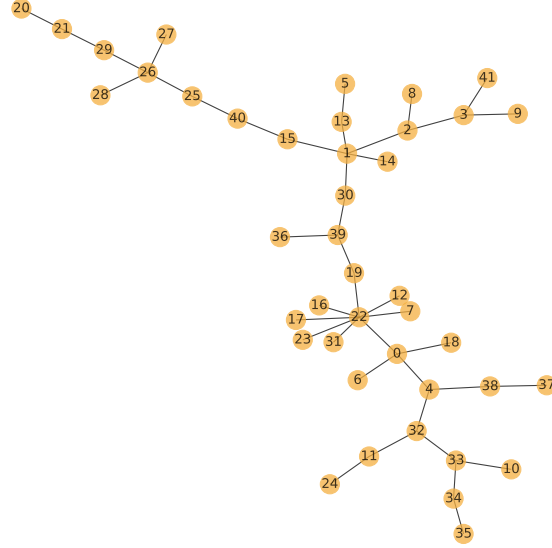


Figure 10: Marginal and pairwise mutual information similarity zoomed in for MST and PATE-GAN for different ϵ levels, on *Census*, varying n .

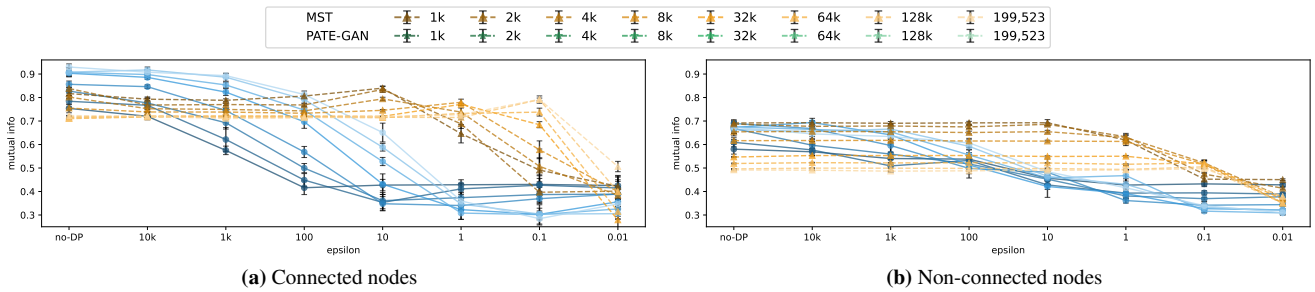


(a) PrivBayes



(b) MST

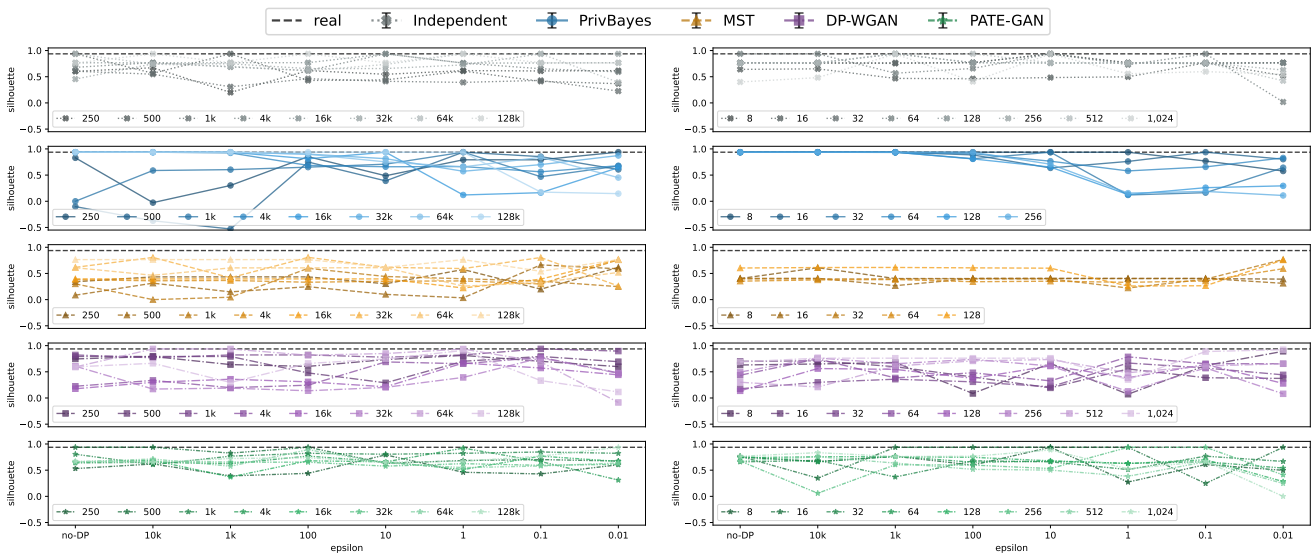
Figure 11: Example fitted networks for PrivBayes and MST with $\epsilon = 1$, on *Census*.



(a) Connected nodes

(b) Non-connected nodes

Figure 12: Pairwise mutual information (connected/non-connected nodes extracted from the fitted networks for PrivBayes and MST) similarity for different ϵ levels, on *Census*, varying n .



(a) Varying n and $d = 32$

(b) Varying n and $d = 32$

Figure 13: Silhouette score for different ϵ levels, on *Mix Gauss Unsup*, varying n and d .

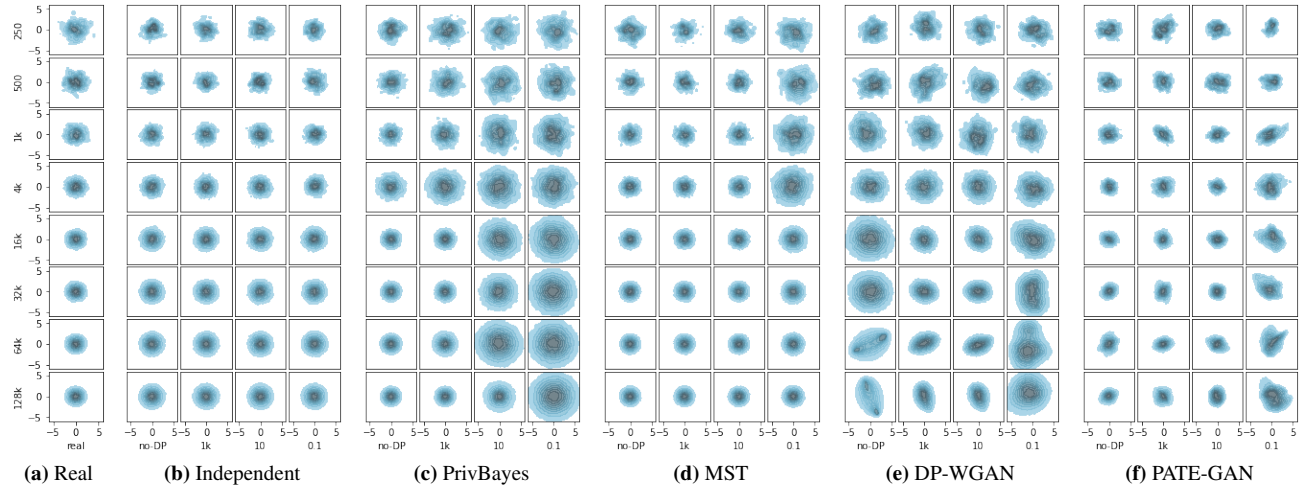


Figure 14: KDE on the first 2 PCA principles for different ϵ levels, on *Eye Gauss*, varying n .

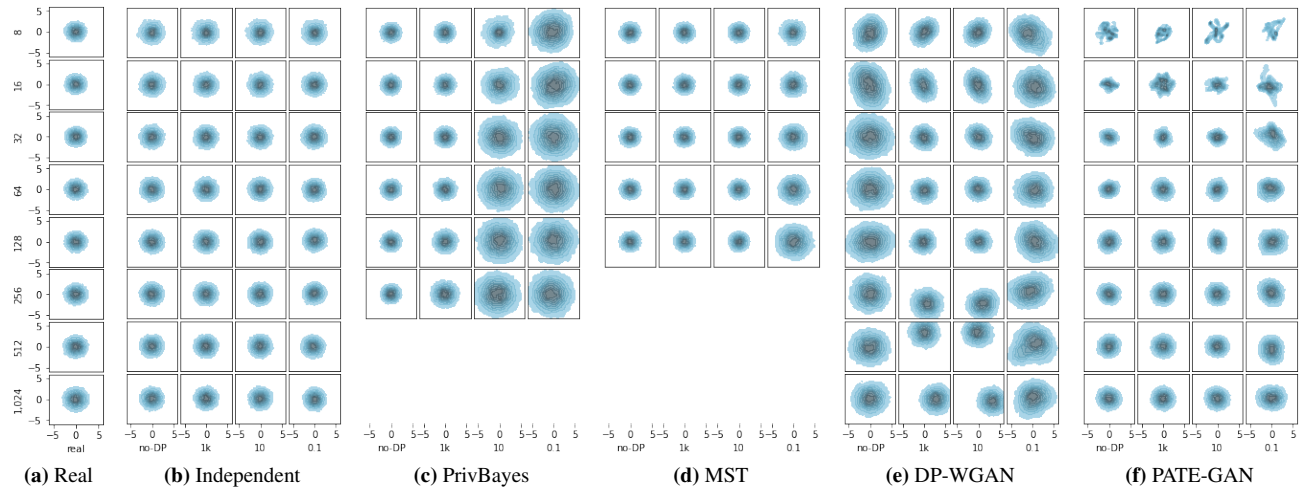


Figure 15: KDE on the first 2 PCA principles for different ϵ levels, on *Eye Gauss*, varying d .

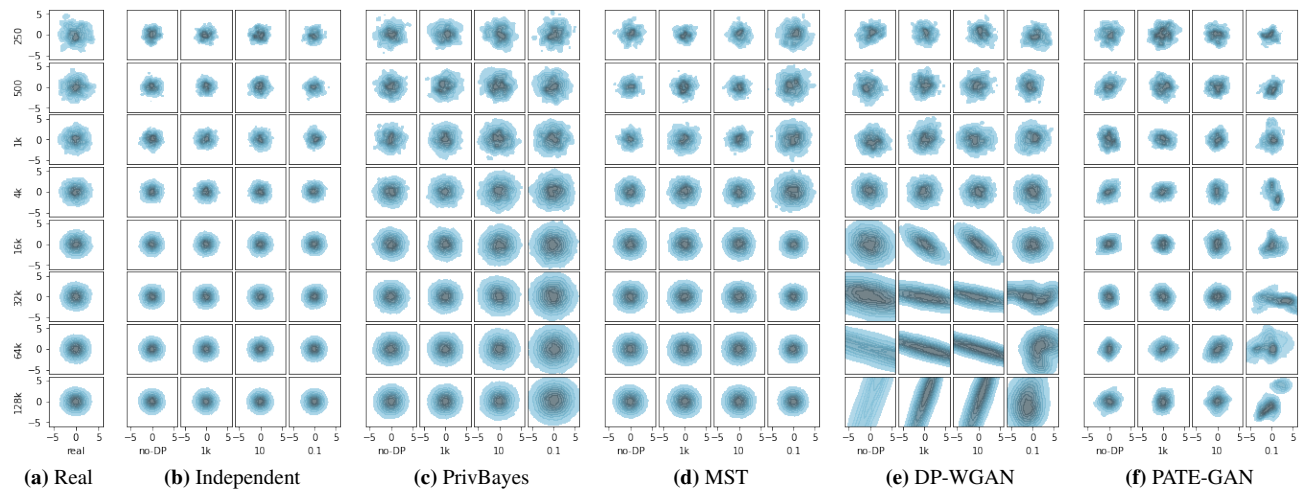


Figure 16: KDE on the first 2 PCA principles for different ϵ levels, on *Corr Gauss*, varying n .

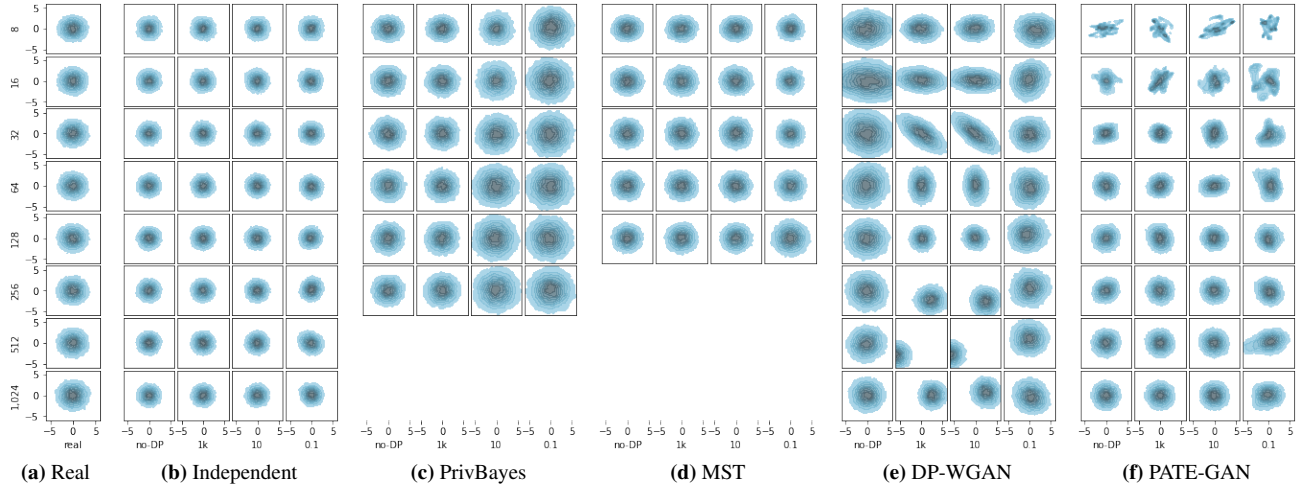


Figure 17: KDE on the first 2 PCA principles for different ϵ levels, on *Corr Gauss*, varying d .

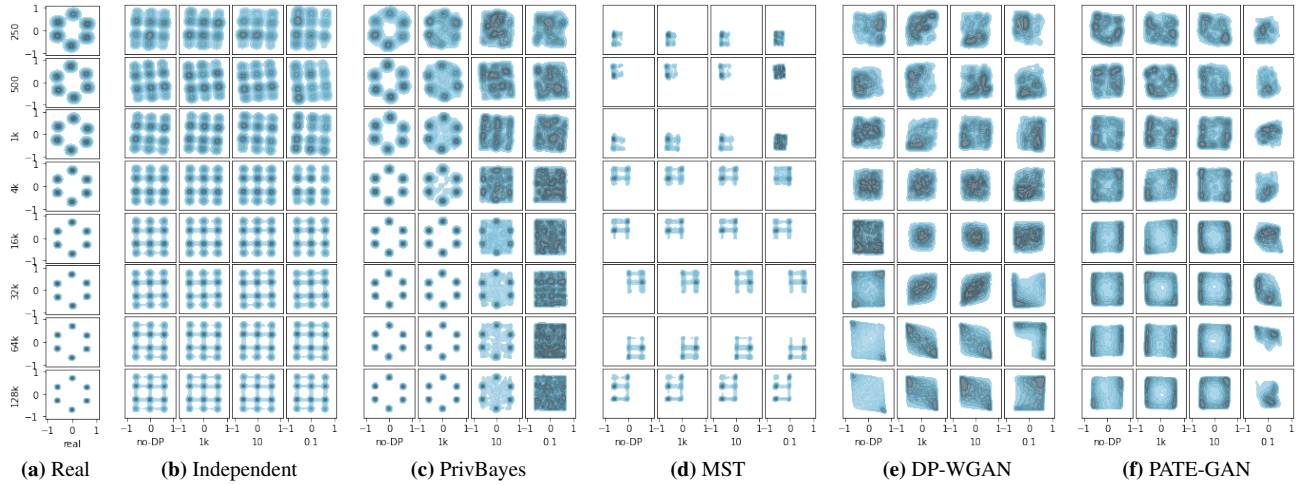


Figure 18: KDE on the first 2 PCA principles for different ϵ levels, on *Mix Gauss Unsup*, varying n .

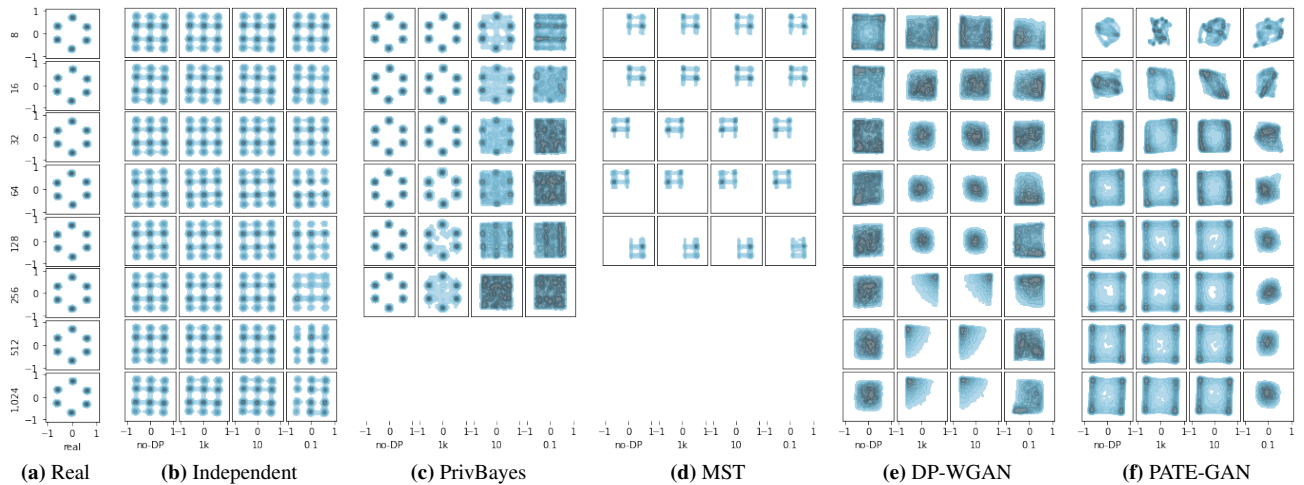


Figure 19: KDE on the first 2 PCA principles for different ϵ levels, on *Mix Gauss Unsup*, varying d .

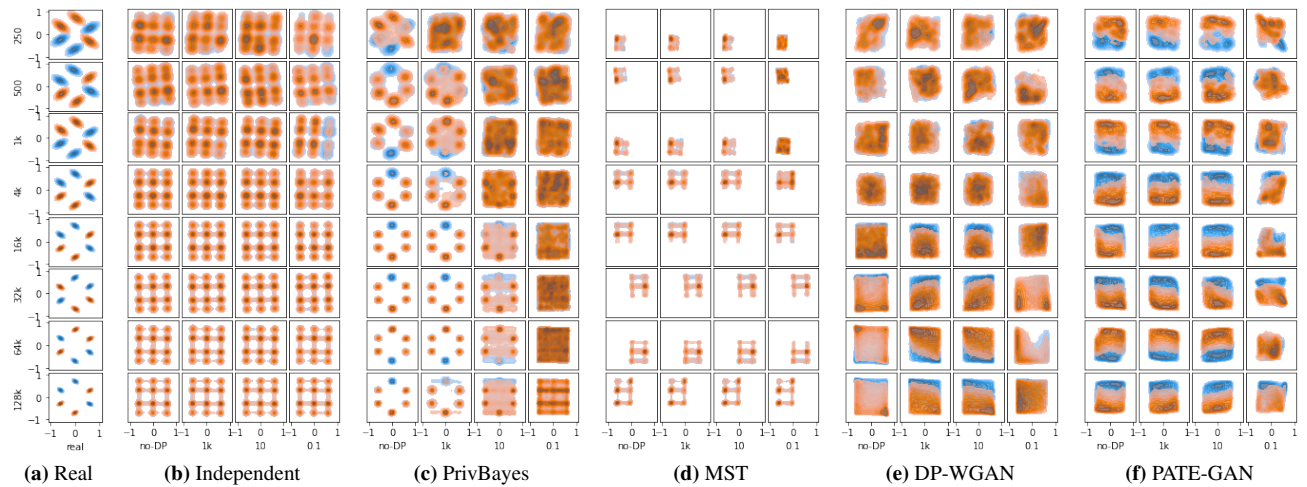


Figure 20: KDE on the first 2 PCA principles for different ϵ levels, on *Mix Gauss Sup*, varying n .

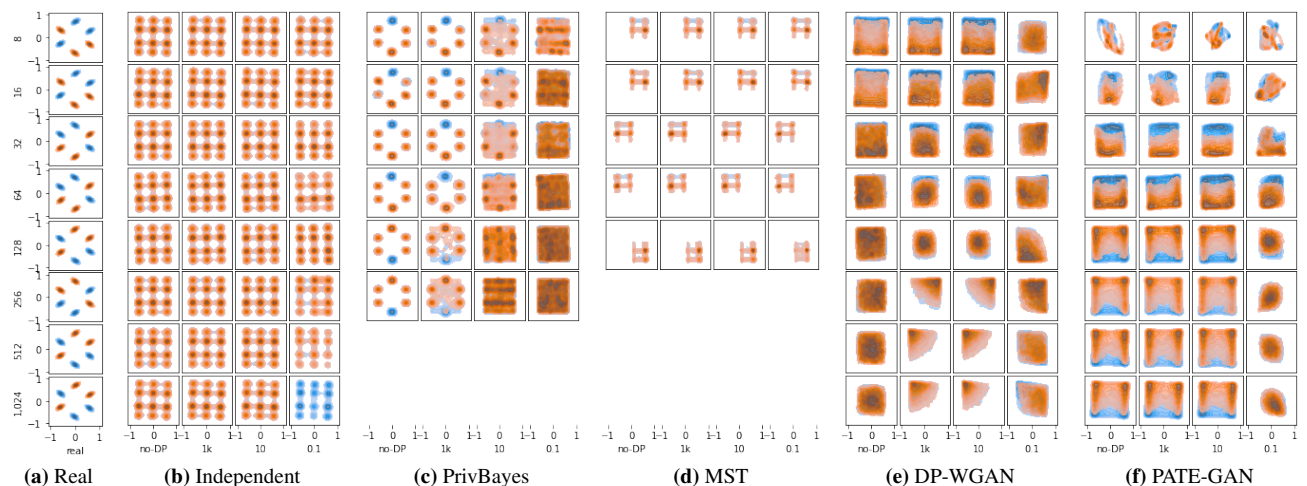
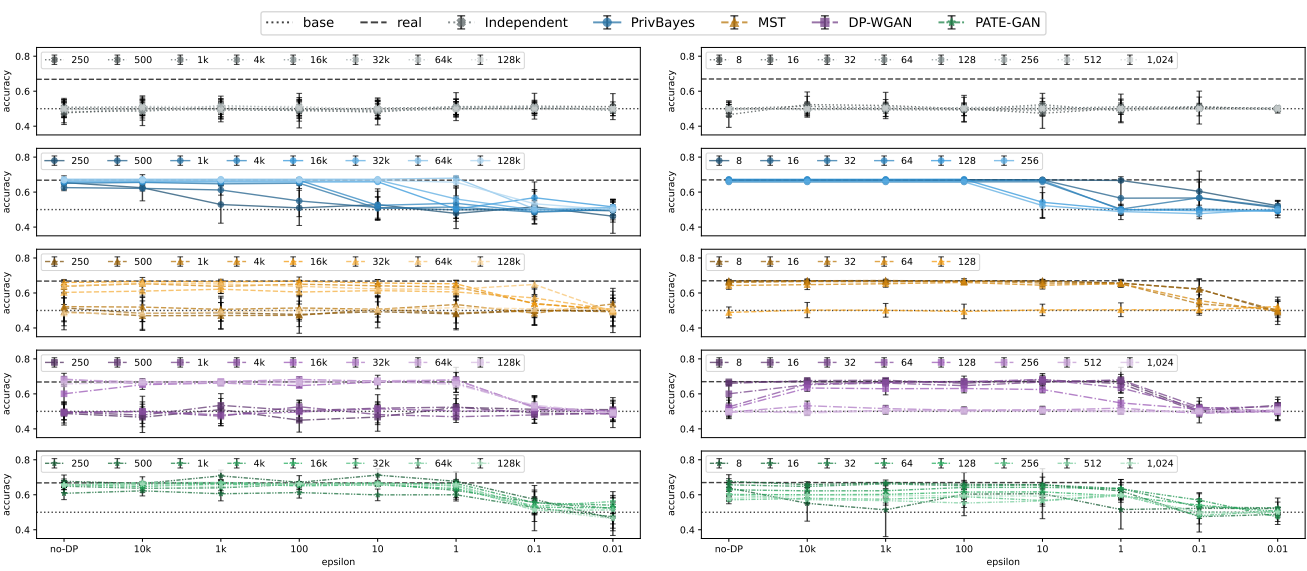


Figure 21: KDE on the first 2 PCA principles for different ϵ levels, on *Mix Gauss Sup*, varying d .



(a) Varying n and $d = 32$

(b) Varying d and $n = 16k$

Figure 22: Accuracy for different ϵ levels, on *Mix Gauss Sup*, varying n and d .

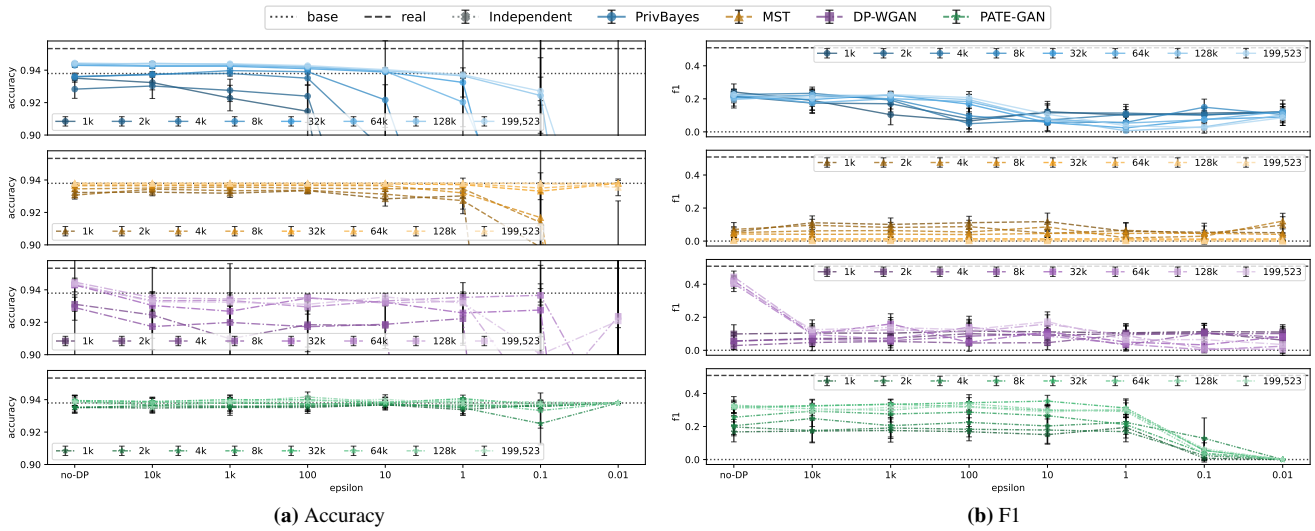


Figure 23: Accuracy and F1 for different ϵ levels, on *Census*, varying n .

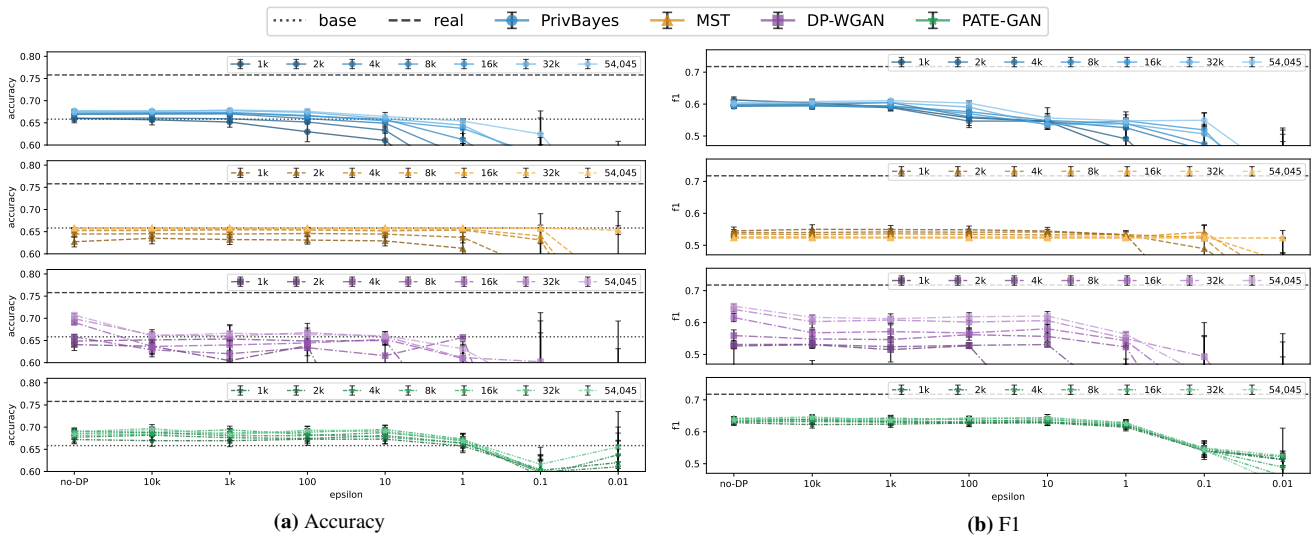


Figure 24: Accuracy and F1 for different ϵ levels, on *Connect 4*, varying n .